Universitat de Girona

# NEW MONO- AND DINUCLEAR RUTHENIUM COMPLEXES CONTAINING THE 3,5-BIS(2-PYRIDYL)PYRAZOLE LIGAND. SYNTHESIS, CHARACTERIZATION AND APPLICATIONS

Cristina SENS LLORCA

**Universitat de Girona**
**Departament de Química**
**Àrea de Química Inorgànica**

# New mono- and dinuclear ruthenium complexes containing the 3,5-bis(2-pyridyl)pyrazole ligand. Synthesis, characterization and applications

**PhD Dissertation presented by**

**CRISTINA SENS LLORCA**

**In Candidacy for the Degree of**

*Doctor of Philosophy in Chemistry*

Girona, January 2005

**Universitat de Girona**

Departament de Química
Àrea de Química Inorgànica

Els sotasignats *Antoni Llobet i Dalmases*, *Isabel Romero García* i *Montserrat Rodríguez Pizarro*, Professor Catedràtic, Professora Titular i Professora A3TC de l'Àrea de Química Inorgànica de la Universitat de Girona respectivament,

CERTIFIQUEM que la memòria que porta per títol **"New mono- and dinuclear ruthenium complexes containing the 3,5-bis(2-pyridyl)pyrazole ligand. Synthesis, characterization and applications"** aplega el treball realitzat sota la nostra direcció per la *Cristina Sens Llorca*, llicenciada en Química, i constitueix la seva memòria per optar al grau de Doctora en Química.

I perquè consti a efectes legals, signem aquest certificat.

Girona, 11 de Gener de 2005

Prof. Dr. Antoni Llobet i Dalmases                    Dra. Isabel Romero García

Dra. Montserrat Rodríguez Pizarro

A la meva família,

A en Josep,

# Agraïments/Acknowledgements

La realització d'una tesi doctoral és un treball complex que no seria possible sense la unió de moltes voluntats. En el transcurs d'aquests quatre anys he contret deutes de gratitud amb moltes persones a les que m'agradaria expressar, des d'aquestes pàgines, el meu sincer agraïment.

Sense més preàmbuls començaré per donar les gràcies als meus directors de tesi. A en Toni li vull agrair que em donés l'oportunitat de realitzar una tesi doctoral sota la seva direcció, i l'esforç i dedicació que li ha suposat la supervisió d'aquesta. A la Marisa, els seus ànims constants, la seva sinceritat i els seus consells. A la Montse li vull agrair que sempre m'hagi dedicat temps quan l'he necessitada, és molt reconfortant tenir a qui recórrer en els moments de *crisi*; gràcies per facilitar-me el camí tantes vegades!

Sempre guardaré un molt bon record d'aquesta etapa de doctorat i tinc la convicció que això ho dec, en gran part, als meus companys i ex-companys de l'àrea d'inorgànica (en Raül, en Xavi, l'Ester, la Isabel, en Quim, l'Arnau, l'Anna, en Xavi Ribes, la Sílvia, en Nadal, la Carme, la Vero i en Jordi). Només dir-vos que ha estat un plaer compartir l'experiència del doctorat amb vosaltres i que us trobaré molt a faltar. A tu Isabel, a més, et vull agrair que em vinguessis a veure als EU; sempre recordaré l'experiència a NY com una de les més maques de la meva vida (*I also love you babe!*). Faig extensiu també el meu agraïment als altres dos professors del grup: a la Mª Ángeles, *por tu buen humor, por tus ánimos y por preguntarme siempre cómo voy*; i a en Miquel, pel seu esperit pedagògic i pels seus consells.

A la resta de companys del departament, amb qui he compartit tants cafès i sopars, gràcies per fer-me la feina més amena i per la vostra ajuda desinteressada quan ha calgut. Vull agrair especialment l'ajuda de l'Eduard i d'en Pedro, dos químics físics, en la realització d'alguns dels càlculs que figuren en aquest treball. Gràcies també a la resta de personal de la Universitat de Girona; laborants, conserges, informàtics, personal de fotocòpies,...A en Jordi Benet-Buchholz per la resolució de les estructures de raig-X, i a en Teo Parella pels espectres de RMN.

I would also like to thank Robert Crabtree and Gary Brudvig from Yale University for allowing me to stay in their group for a research stage. Thanks especially to Sid and Chin-Hin, my Indian and Chinese lab mates. Sid, I don't exaggerate if I say you're the kindest person I have ever met. Thank you for all your help, for my birthday dinner, for the water melons, for your car rides, for the muffins and a long etcetera. I'm glad we keep in contact and don't forget we have to meet again, either in Spain or in India. Chin-Hin, thank you for your friendship and your talks, you did my stage at Yale much more enjoyable.

Em sento molt afortunada d'haver pogut compartir la meva experiència als EU amb la Susana, una estudiant de doctorat de Madrid amb qui per atzar vaig coincidir en la meva estada. Susana, sin duda hiciste el estar lejos muchísimo más fácil, gracias por todo, no pudiste haber sido mejor compañera. Te deseo mucha suerte con tu tesis, ánimo que ya queda poco.

Passant al tema financer, m'agradaria agrair a la UdG la concessió d'una beca predoctoral durant el meu primer any de recerca, i al CIRIT de la Generalitat de Catalunya, la concessió d'una beca predoctoral FI2002.

Per últim, m'agradaria agrair el suport dels amics i la família. A les meves amigues, l'Anna Alejo, la Mireia, la Nuri, la Gemma, la Lídia i l'Anna Ros, companyes de confidències i nits de marxa, per la seva amistat i per fer-me veure que la química no és el més important; no canvieu mai! Vull donar les gràcies molt especialment a la meva família, per estimar-me, recolzar-me, aconsellar-me, per preocupar-se i per respectar sempre les meves decisions. Sens dubte sou qui més mereix el meu agraïment i aquesta tesi va dedicada a vosaltres.

I a tu Josep, algú va dir que el més important no és el que fas a la vida sinó qui t'acompanya; m'alegro molt que siguis tu. Gràcies per tot.

# Graphical Abstracts

## I – INTRODUCTION (pages 1–36)
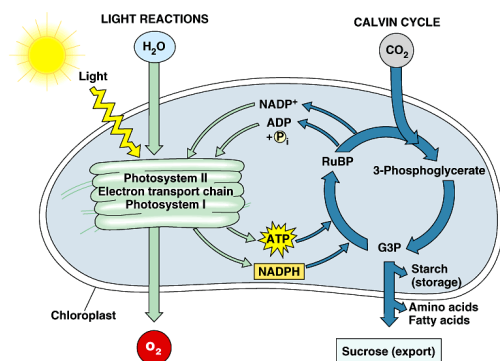


> *"…the fundamental problem from the technical point of view is how to fix the solar energy through suitable photochemical reactions. To do this it would be sufficient to be able to imitate the assimilating processes of plants. As is well known, plants transform the carbon dioxide of the atmosphere into starch, setting free oxygen. …By using suitable catalyzers, it should be possible to transform the mixture of water and carbon dioxide into oxygen and methane, or to cause other endo-energetic processes."*
>
> **Giacomo Ciamician**
> *Science* 1912

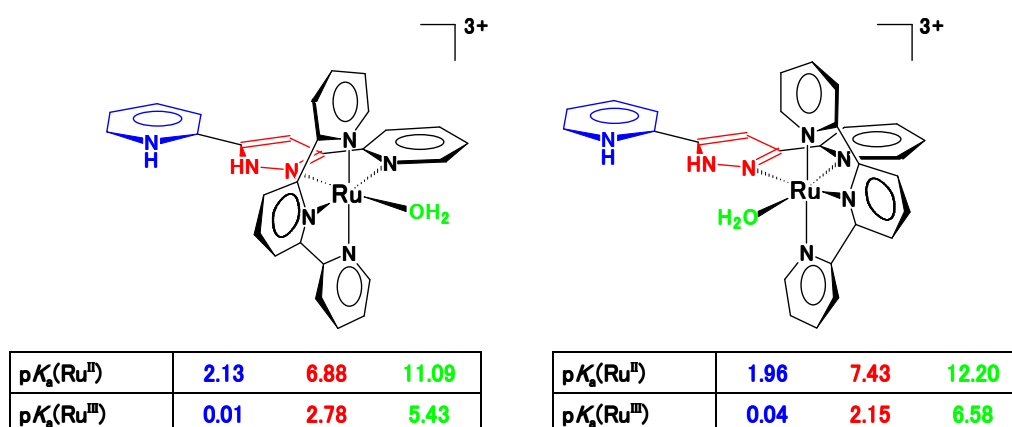## II – OBJECTIVES (pages 37–40)

## III – PUBLICATIONS (pages 43–176)

**Paper A (pages 45–68).** *Synthesis, Structure, and Spectroscopic, Photochemical, Redox, and Catalytical Properties of Ruthenium(II) Isomeric Complexes Containing Dimethyl Sulfoxide, Chloro, and the Dinucleating Bis(2-pyridyl)pyrazole Ligands*
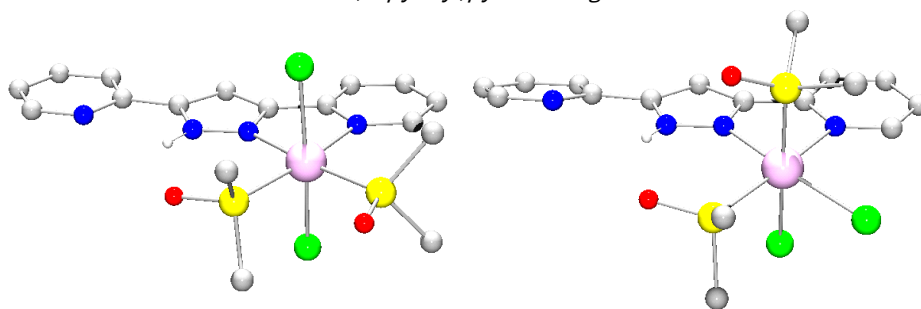


Two isomeric Ru(II) complexes containing the dinucleating Hbpp (3,5-bis(2-pyridyl)pyrazole) ligand together with Cl and dmso ligands have been prepared and their structural, spectroscopic, electrochemical, photochemical, and catalytic properties studied. The crystal structures of *trans,cis*-[Ru$^{II}$Cl$_2$(Hbpp)(dmso)$_2$], **2a,** and *cis(out),cis*-[Ru$^{II}$Cl$_2$(Hbpp)(dmso)$_2$], **2b**, have been solved by means of single-crystal X-ray diffraction analysis showing a distorted octahedral geometry for the metal center where the dmso ligands coordinate through their S atom. 1D and 2D NMR spectroscopy corroborates a similar structure in solution for both isomers. Exposure of either **2a** or **2b** in acetonitrile solution under UV light produces a substitution of one dmso ligand by a solvent molecule generating the same product namely, *cis(out)*-[Ru$^{II}$Cl$_2$(Hbpp)(MeCN)(dmso)], **4**. While the 1 e$^-$ oxidation of **2b** or *cis(out),cis*-[Ru$^{II}$Cl$_2$(bpp)(dmso)$_2$]$^+$, **3b**, generates a stable product, the same process for **2a** or *trans,cis*-[Ru$^{II}$Cl$_2$(bpp)(dmso)$_2$]$^+$, **3a**, produces the interesting linkage isomerization phenomenon where the dmso ligand switches its bond from Ru–S to Ru–O ($K^{III}_{O \to S} = 0.25 \pm 0.025$, $k^{III}_{O \to S} = 0.017$ s$^{-1}$, and $k^{III}_{S \to O} = 0.065$ s$^{-1}$; $K^{II}_{O \to S} = 6.45 \times 10^9$, $k^{II}_{O \to S} = 0.132$ s$^{-1}$, $k^{II}_{S \to O} = 2.1 \times 10^{-11}$ s$^{-1}$). Finally complex **3a** presents a relatively high activity as hydrogen transfer catalyst, with regard to its ability to transform acetophenone into 2-phenylethyl alcohol using 2-propanol as the source of hydrogen atoms.

**Paper B (pages 71–116).** *Synthesis, Structure, and Acid–Base and Redox Properties of a Family of New Ru(II) Isomeric Complexes Containing the Trpy and the Dinucleating Hbpp Ligands*

| p$K_a$(Ru$^{II}$) | 2.13 | 6.88 | 11.09 |
|---|---|---|---|
| p$K_a$(Ru$^{III}$) | 0.01 | 2.78 | 5.43 |

| p$K_a$(Ru$^{II}$) | 1.96 | 7.43 | 12.20 |
|---|---|---|---|
| p$K_a$(Ru$^{III}$) | 0.04 | 2.15 | 6.58 |

Three pairs of mononuclear geometrical isomers containing the ligand 3,5–bis(2–pyridyl)pyrazole (Hbpp) of general formula *in*– and *out*–[Ru$^{II}$(Hbpp)(trpy)X]$^{n+}$ (trpy = 2,2':6',2''–terpyridine; X = Cl, $n$ = 1, **2a,b**; X = H$_2$O, $n$ = 2, **3a,b**; X = py (pyridine), $n$ = 2, **4a,b**) have been prepared through two different synthetic routes, isolated, and structurally characterized. The solid state structural characterization was performed by X–ray diffraction analysis of four complexes: **2a–4a** and **4b**. The structural characterization in solution was performed by means of 1D and 2D NMR spectroscopy for complexes **2a,b** and **4a,b** and coincides with the structures found in the solid state. All complexes were also spectroscopically characterized by UV–vis which also allowed us to carry out spectrophotometric acid–base titrations. Thus, a number of species were spectroscopically characterized with the same oxidation state but with a different degree of protonation. As an example, for **3a** three p$K_a$ values were obtained: p$K_{a1}$(Ru$^{II}$) = 2.13, p$K_{a2}$(Ru$^{II}$) = 6.88, and p$K_{a3}$(Ru$^{II}$) = 11.09. The redox properties were also studied, giving in all cases a number of electron transfers coupled to proton transfers. The pH dependency of the redox potentials allowed us to calculate the p$K_a$ of the complexes in the Ru(III) oxidation state. For complex **3a**, these were found to be p$K_{a1}$(Ru$^{III}$) = 0.01, p$K_{a2}$(Ru$^{III}$) = 2.78, and p$K_{a3}$(Ru$^{III}$) = 5.43. The oxidation state Ru(IV) was only reached from the Ru–OH$_2$ type of complexes **3a** or **3b**. It has also been shown that the Ru$^{IV}$=O species derived from **3a** is capable of electrocatalytically oxidizing benzyl alcohol with a second–order rate constant of $k_{cat}$ = 17.1 M$^{-1}$ s$^{-1}$.

**Paper C (pages 119–122).** *A New Ru Complex Capable of Catalytically Oxidizing Water to Molecular Dioxygen*
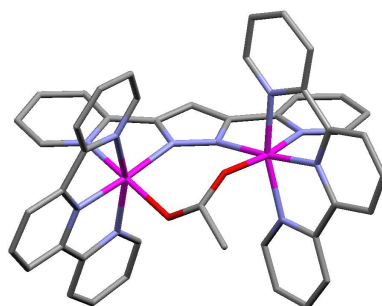
We have prepared three new dinuclear ruthenium complexes having the formulas [Ru$^{II}_2$(bpp)(trpy)$_2$(μ–L)]$^{2+}$ (L = Cl, **1**; L = AcO, **2**) and [Ru$^{II}_2$(bpp)(trpy)$_2$(H$_2$O)$_2$]$^{3+}$ (**3**). The three complexes have been characterized through the usual spectroscopic and electrochemical techniques and, in the cases of **1** and **2**, the X–ray crystal structures have been solved. In aqueous acidic solution, the acetato bridge of **2** is replaced by aqua ligands, generating the bis(aqua) complex **3** which, upon oxidation to its Ru$^{IV}$Ru$^{IV}$ state, has been shown to catalytically oxidize water to molecular dioxygen. The measured pseudo–first–order rate constant for the O$_2$–evolving process is $1.4 \times 10^{-2}$ s$^{-1}$, more than 3 times larger than the higher one previously reported for Ru–O–Ru type catalysts. This new water splitting catalyst also has improved stability with regard to any previously described, achieving a total of 18.6 metal cycles.
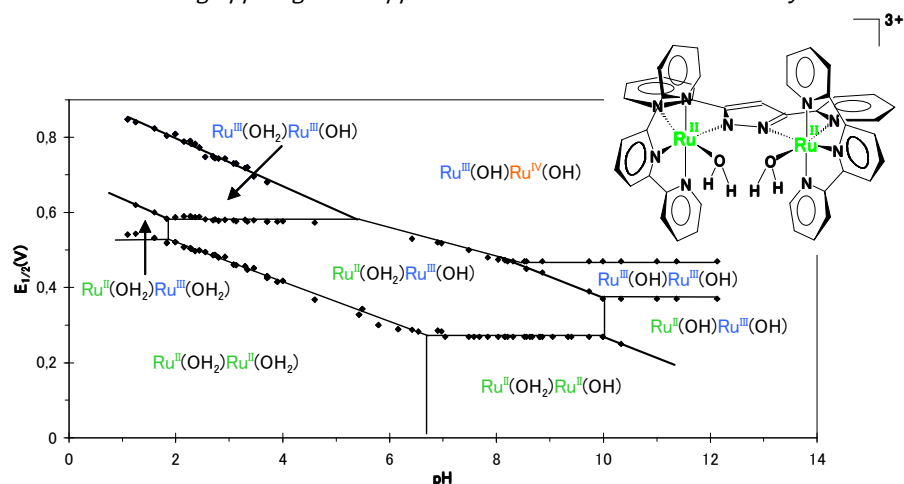
Two new ruthenium dimers containing the dinucleating 3,5–bis(2–pyridyl)pirazolate (bpp⁻) and trpy ligands have been synthesized and characterized by means of structural, spectroscopic and electrochemical techniques. These complexes have the formula $[Ru_2(\mu–X)(bpp)(trpy)_2]^{2+}$, where X = Cl, **1**, and acetate, **2**. The chloro and acetato bridges can be hydrolyzed in basic and acidic media, respectively, to generate the diaqua analog $[Ru_2(bpp)(trpy)_2(H_2O)_2]^{3+}$, **3**, which has also been thoroughly characterized. This complex has been shown to catalytically oxidize water to molecular dioxygen when oxidized to the $Ru^{IV}–Ru^{IV}$ state, either in homogeneous solution or in a heterogeneous Nafion membrane. The yields of $O_2$ in the membrane, however, are lower than those in solution. Kinetic studies, performed in acidic aqueous solution, show that the initial $O_2$ evolution rate is first order with respect to the complex concentration. The pseudo–first–order rate constant ($k_{O2}$ (s⁻¹)) for $O_2$ evolution has been calculated as $1.4 \times 10^{-2}$, which is among the highest values reported up to date. Although the complex presents improved stability with regard to previously described homogeneous catalysts, it still deactivates in the course of the catalysis to yield a compound whose nature we are currently trying to elucidate.

# Table of Contents

# Glossary of Terms and Abbreviations

| | |
|---|---|
| δ | chemical shift (units: ppm) |
| ν (in IR) | frequency (units: $cm^{-1}$) |
| Ar | aryl |
| BOC | *tert*-butyloxycarbonyl |
| bpy | 2,2'-bipyridine |
| Bu | butyl |
| cat. | catalyst |
| COSY | correlation spectroscopy |
| CV | cyclic voltammetry |
| D1/2 | reaction center core proteins of photosystem II |
| dmso | dimethyl sulfoxide |
| $E^0$ | standard redox potential |
| $E_{1/2}$ | half-wave potential |
| $E_{p,a}$ | anodic peak potential |
| $E_{p,c}$ | cathodic peak potential |
| EPR | electron paramagnetic resonance |
| ESI-MS | electrospray ionization mass spectrometry |
| EtOAc | ethyl acetate |
| EXAFS | extended X-ray absorption fine structure |
| FT-IR | fourier transform infrared spectroscopy |
| GC-MS | gas chromatography-mass spectrometry |
| Hbpp | 3,5-bis(2-pyridyl)pyrazole |
| HETCOR | heteronuclear chemical shift correlation |
| J | coupling constant |
| $K_a$ | acidity constant |
| $K^{III}_{O \rightarrow S}/K^{II}_{O \rightarrow S}$ | equilibrium constants for the linkage isomerization of *O*-dmso to *S*-dmso in Ru(III)/Ru(II) complexes |
| $k^{III}_{O \rightarrow S}/k^{II}_{O \rightarrow S}$ | kinetic constants for the linkage isomerization of *O*-dmso to *S*-dmso in Ru(III)/Ru(II) complexes |
| $k^{III}_{S \rightarrow O}/k^{II}_{S \rightarrow O}$ | kinetic constants for the linkage isomerization of *S*-dmso to *O*-dmso in Ru(III)/Ru(II) complexes |
| $k_{O2}$ ($s^{-1}$) | pseudo-first-order rate constant for $O_2$ evolution |
| M | molar |

| | |
|---|---|
| **m (in IR)** | medium |
| **m/z** | mass-to-charge ratio |
| **Me** | methyl |
| **MLCT** | metal-to-ligand charge-transfer |
| **MS** | mass spectrometry |
| **NADP$^+$/NADPH** | oxidized/reduced form of nicotinamide adenine dinucleotide phosphate |
| **NMR** | nuclear magnetic resonance |
| **NOE** | nuclear overhauser effect |
| **NOESY** | nuclear overhauser spectroscopy |
| **OAc** | acetate |
| ***O*-dmso** | oxygen-bonded dimethyl sulfoxide |
| **OEC** | oxygen-evolving complex |
| **ORTEP** | Oak Ridge thermal ellipsoid plot |
| **oxone** | peroxymonosulfate, $HSO_5^-$ |
| **Ph** | phenyl |
| **ppm** | parts per million |
| **PSI** | photosystem I |
| **PSII** | photosystem II |
| **py** | pyridine |
| **s (in IR)** | strong |
| ***S*-dmso** | sulfur-bonded dimethyl sulfoxide |
| **SSCE** | sodium saturated calomel electrode |
| **TBAH** | tetrabutylammonium hexafluorophosphate |
| **TMS** | tetramethylsilane |
| **trpy** | 2,2':6',2"-terpyridine |
| **UV-vis** | ultraviolet-visible spectroscopy |
| **w (in IR)** | weak |
| **XANES** | X-ray absorption near edge structure |
| **$v_{O2}$ (mol s$^{-1}$)** | initial oxygen evolution rate |

**Multiplicity of signals in NMR spectra:**

| | |
|---|---|
| **d** | doublet |
| **dd** | doublet of doublets |
| **ddd** | doublet of doublets of doublets |
| **s** | singlet |
| **t** | triplet |
| **td** | triplet of doublets |

# Supplementary Digital Material

The material listed below can be found in the attached CD:

- pdf file of the PhD dissertation

- cif files for each crystal structure presented within this thesis

| Crystal structure | File Name |
|---|---|
| *trans,cis*–[RuCl$_2$(Hbpp)(dmso)$_2$]·MeOH | trans–Cl |
| *cis(out),cis*–[RuCl$_2$(Hbpp)(dmso)$_2$] | cis–Cl |
| *out*–[RuCl(H$_2$bpp)(trpy)]Cl(PF$_6$)·4.63H$_2$O | out–Cl |
| *out*–[Ru(Hbpp)(trpy)(H$_2$O)](ClO$_4$)$_2$·3H$_2$O | out–aqua |
| *out*–[Ru(py)(Hbpp)(trpy)](PF$_6$)$_2$·H$_2$O | out–py |
| *in*–[Ru(py)(Hbpp)(trpy)](PF$_6$)$_2$·MeCN | in–py |
| [Ru$_2$(μ–Cl)(bpp)(trpy)$_2$](PF$_6$)$_2$ | dimer–Cl |
| [Ru$_2$(μ–O$_2$CMe)(bpp)(trpy)$_2$](PF$_6$)$_2$·2MeCOMe | dimer–acetato |
| [Ru$_2$(bpp)(OH)(trpy)$_2$(H$_2$O)](PF$_6$)$_2$·Me$_2$CO·Et$_2$O | dimer–aqua |
| [Ru$_2$(μ–O$_2$CCF$_3$)(bpp)(trpy)$_2$](PF$_6$)$_2$·CH$_2$Cl$_2$ | dimer–trifluoroacetato |

# INTRODUCTION
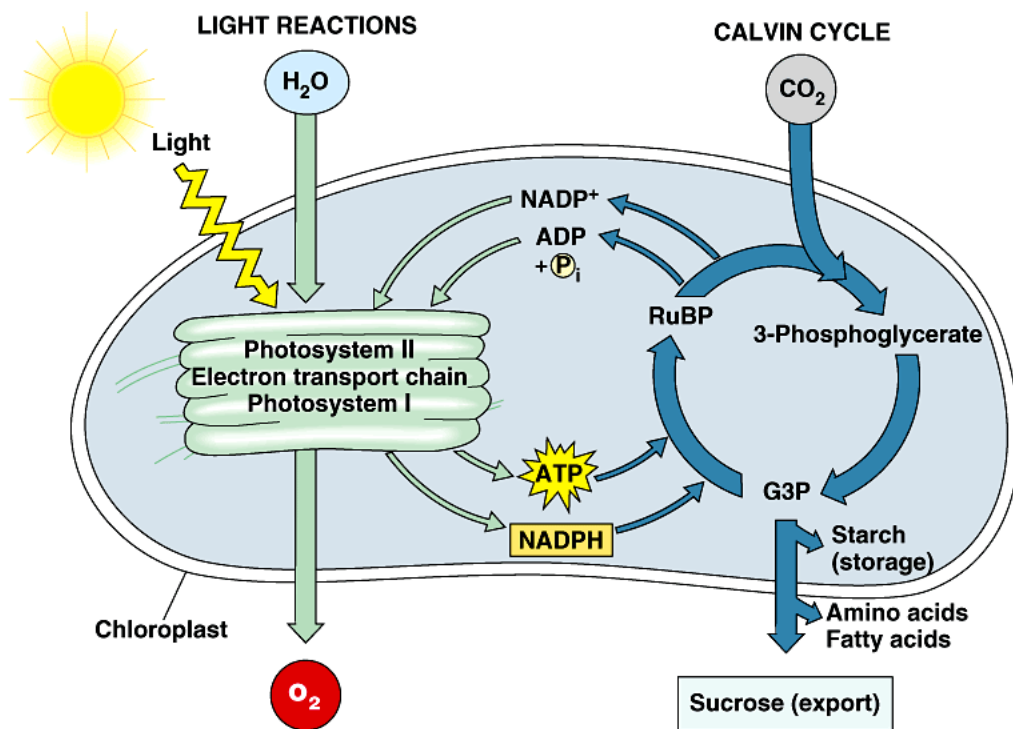


"…the fundamental problem from the technical point of view is how to fix the solar energy through suitable photochemical reactions. To do this it would be sufficient to be able to imitate the assimilating processes of plants. As is well known, plants transform the carbon dioxide of the atmosphere into starch, setting free oxygen.

…By using suitable catalyzers, it should be possible to transform the mixture of water and carbon dioxide into oxygen and methane, or to cause other endo-energetic processes."

**Giacomo Ciamician**
*Science* 1912

# TABLE OF CONTENTS

## 1- An introduction to ruthenium chemistry.

The chemistry of ruthenium complexes, with special attention to their electron-transfer properties, has been receiving continuous attention for the latest decades. Ruthenium offers a wide range of oxidation states which are accessible chemically and electrochemically (from oxidation state $-2$ in $[Ru(CO)_4]^{2-}$ to $+8$ in $RuO_4$). Therefore, the complexes of ruthenium are redox-active and their application as redox reagents in different chemical reactions is of much current interest. The kinetic stability of ruthenium in several different oxidation states, the often reversible nature of its redox couples, and the relative ease with which mixed-ligand complexes can be prepared by controllable stepwise methods, all make ruthenium complexes particularly attractive targets of study.

Ruthenium complexes exhibit a great deal of applications in many fields of chemistry. Clear correlations can be observed between their properties and the nature of the ligands bound to the central ion. Thus, ruthenium sulfoxide complexes have been extensively investigated in the last two decades because of their properties and usefulness, particularly in catalysis[1] and chemotherapy.[2] Ruthenium complexes with polypyridyl ligands have received much attention owing to their interesting spectroscopic, photophysical, photochemical and electrochemical properties, which lead to potential uses in diverse areas such as photosensitizers for photochemical conversion of solar energy,[3] molecular

[1] Kagan, H. B.; Ronan, B. *Reviews on Heteroatom Chem.* **1992**, *7*, 92–116.

[2] (a) Alessio, E.; Mestroni, G.; Bergamo, A.; Sava, G. in "Metal Ions and Their Complexes in Medication and in Cancer Diagnosis and Therapy", Vol. 42 of *Met. Ions Biol. Syst.*, A. Sigel and H. Sigel eds., M. Dekker: New York, 2004, p. 323–351. (b) Galanski, M.; Arion, V. B.; Jakupec, M. A.; Keppler, B. K. *Curr. Pharm. Des.* **2003**, *9*, 2078–2089. (c) Clarke, M. J.; Zhu, F.; Frasca, D. R. *Chem. Rev.* **1999**, *99*, 2511–2533. (d) Sava, G.; Alessio, E.; Bergamo, A.; Mestroni, G. in "Sulfoxide ruthenium complexes: non toxic tool for the selective treatment of solid tumour metastases", Vol. 1 of *Topics in Biological Inorganic Chemistry*, "*Metallo-pharmaceuticals*", M. J. Clarke and P. J. Sadler eds., Springer, Berlin, 1999, p. 143–169. (e) Mestroni, G.; Alessio, E.; Sava, G.; Pacor, S.; Coluccia, M. in *Metal Complexes in Cancer Chemotherapy*, B. K. Keppler eds., VCH Verlag, Weinheim, 1994, p. 159. (f) Mestroni, G.; Alessio, E.; Sava, G.; Pacor, S.; Coluccia, M.; Boccarelli, A. *Metal-Based Drugs* **1994**, *1*, 41–63.

[3] (a) Islam, A.; Sugihara, H.; Arakawa, H. *J. Photochem. and Photobiol. A-Chemistry* **2003**, *158*, 131–138. (b) Hammarstrom, L.; Sun, L. C.; Akermark, B.; Styring, S. *Catal. Today* **2000**, *58*, 57–69. (c) Kalyanasundaram, K.;

electronic devices[4] and as photoactive DNA cleavage agents for therapeutic purposes.[5] These polypyridylic complexes are also known to perform a variety of inorganic and organic transformations. Their synthetic versatility, high catalytic performance under relatively mild reaction conditions, and high selectivity make these complexes particularly well suited for this purpose. In particular, polypyridyl complexes of ruthenium with aqua ligands are used extensively for the oxidation of organic substrates, and multiple oxidative pathways have been detected including atom transfer, C–H insertion, and proton–coupled electron transfer.[6]

A large number of novel organic reactions has also been described using ruthenium catalysts with carbonyl, tertiary phosphines, cyclopentadienyl, arene/dienes, and carbenes

Gratzel, M. *Coord. Chem. Rev.* **1998**, *177*, 347–414. (d) Balzani, V.; Juris, A.; Ventura, M.; Campagna, S.; Serroni, S. *Chem. Rev.* **1996**, *96*, 759. (e) Meyer, T. J. *Pure Appl. Chem.* **1990**, *62*, 1003. (f) Meyer, T. J. *Acc. Chem. Res.* **1989**, *22*, 163. (g) Juris, A.; Balzani, V.; Barigelletti, F.; Campagna, S.; Belser, P.; von Zelewsky, A. *Coord. Chem. Rev.* **1988**, *84*, 85. (h) Kalyanasundaram, K. *Coord. Chem. Rev.* **1982**, *46*, 159.

[4] (a) Newkome, G. R.; Cho, T. J.; Moorefield, C. N.; Mohapatra, P. P.; Godinez, L. A. *Chem. Eur. J.* **2004**, *10*, 1493–1500. (b) Mishra, L.; Yadaw, A. K.; Govil, G. *Indian J. Chem. Sect A* **2003**, *42*, 1797–1814. (c) Barigelletti, F.; Flamigni, L. *Chem. Soc. Rev.* **2000**, *29*, 1. (d) El–Ghayoury, A.; Harriman, A.; Khatyr, A.; Ziessel, R. *Angew. Chem., Int. Ed. Engl.* **2000**, *39*, 185. (e) Belser, P.; Bernhard, S.; Blum, C.; Beyeler, A.; DeCola, L.; Balzani, V. *Coord. Chem. Rev.* **1999**, *190–192*, 155–169. (f) Venturi, M.; Serroni, S.; Juris, A.; Campagna, S.; Balzani, V. *Top. Curr. Chem.* **1998**, *197*, 193. (g) DeCola, L.; Belser, P. *Coord. Chem. Rev.* **1998**, *177*, 301–346. (h) Balzani, V.; Campagna, S.; Denti, G.; Juris, A.; Serroni, S.; Venturi, M. *Acc. Chem. Res.* **1998**, *31*, 26. (i) Balzani, V.; Juris, A.; Venturi, M.; Campagna, S.; Serroni, S. *Chem. Rev.* **1996**, *96*, 759.

[5] (a) Jiang, C. W.; Chao, H.; Hong, X. L.; Li, H.; Mei, W. J.; Ji, L. N. *Inorg. Chem. Commun.* **2003**, *6*, 773–775. (b) Ossipov, D.; Gohil, S.; Chattopadhyaya, J. *J. Am. Chem. Soc.* **2002**, *124*, 13416–13433. (c) Chao, H.; Mei, W. H.; Huang, Q. W.; Ji, L. N. *J. Inorg. Biochem.* **2002**, *92*, 165–170. (d) Hotze, A. C. G.; Broekhuisen, M. E. T.; Velders, A. H.; Vanderschilden, K.; Haasnoot, J. G.; Reedijk, J. *Eur. J. Inorg. Chem.* **2002**, 369–376. (e) Delaney, S.; Pascaly, M.; Bhattacharya, P. K.; Han, K.; Barton, J. K. *Inorg. Chem.* **2002**, 41, 1966–1974. (f) Liu, J. G.; Ji, L. N. *Chin. J. Inorg. Chem.* **2000**, *16*, 195–203. (g) Hotze, A. C. G.; Velders, A. H.; Vgozzoli, F.; Biaginicingi, M.; Manottilanfredi, A. M.; Haasnoot, J. G.; Reedijk, J. *Inorg. Chem.* **2000**, *39*, 3838–3844. (h) Liu, J. G.; Ye, B. H.; Li, H.; Zhen, Q. X.; Ji, L. N.; Fu, Y. H. *J. Inorg. Biochem.* **1999**, *76*, 265–271. (i) Zhen, Q. X.; Ye, B. H.; Zhang, Q. L.; Liu, J. G.; Li, H.; Ji, L. N.; Wang, L. *J. Inorg. Biochem.* **1999**, *76*, 47–53.

[6] (a) Geneste, F.; Moinet, C. *New J. Chem.* **2004**, *28*, 722–726. (b) Rodríguez, M.; Romero, I.; Llobet, A. *Inorg. Chem.* **2001**, *40*, 4150–4156. (c) Chatterjee, D.; Mitra, A. *Inorg. Chem. Commun.* **2000**, *3*, 640–644. (d) Catalano, V. J.; Heck, R. A.; Öhman, A.; Hill, M. G. *Polyhedron* **2000**, *19*, 1049–1055. (e) Lebeau, E. L.; Meyer, T. J. *Inorg. Chem.* **1999**, *38*, 2174–2181. (f) Nararra, M.; Galembeak, S. E.; Romero, J. R.; Giovani, W. F. D. *Polyhedron* **1996**, *15*, 1531–1537. (g) Gerli, A.; Reedijk, J.; Lakin, M. T.; Spek, A. L. *Inorg. Chem.* **1995**, *34*, 1836–1843. (h) Gerli, A.; Reedijk, J. *J. Mol. Catal. A.: Chem.* **1994**, *89*, 101–112. (i) Cheng, W. C.; Yu, W. Y.; Cheung, K. K.; Che, C. M. *J. Chem. Soc., Dalton Trans.* **1994**, *57*. (j) Griffith, W. P.; Jolliffe, J. M. *J. Chem. Soc., Dalton Trans.* **1992**, 3483. (k) Dengel, A. C.; El–Hendawy, A. M.; Griffith, W. P.; O'Mahoney, C. A.; William, D. J. *J. Chem. Soc., Dalton Trans.* **1990**, 737.

as supporting ligands.[7] These ligands allow the generation of coordinatively unsaturated species and stabilize the reactive intermediates, thus favoring the catalytic process. Organometallic and coordination complexes with different types of ligands also show specific properties in nonlinear optics,[8] magnetism,[9] molecular sensors[10] or liquid crystals.[11]

Some general properties and applications of ruthenium dimethyl sulfoxide complexes and ruthenium polypyridyl complexes with aqua ligands are detailed in this section.

## 1.1- Properties of the Ru-dmso complexes.

Because of the contrasting binding properties of the S and O atoms, dimethyl sulfoxide can form *S*-dmso and *O*-dmso linkage isomers, depending on the nature and characteristics of the transition metal ions. The sulfynil group provides a good acceptor site for π-electron donor species, such as low spin iron(II) and ruthenium(II) ions, while the oxygen atom is the preferred site for hard metals, such as the **3d** trivalent cations, aluminum(III) and lanthanides. While most of the Ru[II] complexes exhibit a great affinity for sulfur ligands, the preference demonstrated by the corresponding Ru[III] species is usually inverted, favoring the binding of the *O*-donor sites.

The ambidentate nature of the dmso ligand is responsible for the linkage isomerism that

[7] (a) Murahashi, S.-I., Takaya, H.; Naota, T. *Pure Appl. Chem.* **2002**, *74*, 19–24. (b) Trost, B. M.; Toste, F. D.; Pinkerton, A. B. *Chem. Rev.* **2001**, *101*, 2067–2096. (c) Naota, T.; Takaya, H.; Murahashi, S.-I. *Chem. Rev.* **1998**, *98*, 2599–2660.

[8] (a) Bella, S. D. *Chem. Soc. Rev.* **2001**, *30*, 355. (b) Whittall, I. R.; McDonagh, A. M.; Humphrey, M. G.; Samoc, M. *Adv. Organomet. Chem.* **1999**, *43*, 349. (c) Whittall, I. R.; McDonagh, A. M.; Humphrey, M. G.; Samoc, M. *Adv. Organomet. Chem.* **1998**, *42*, 291. (d) Verbiest, T.; Houbrechts, S.; Kauranen, M.; Clays, K.; Persoons, A. J. *J. Mater. Chem.* **1997**, *7*, 2175. (e) Long, N. J. *Angew. Chem., Int. Ed. Engl.* **1995**, *34*, 21–38. (f) Nalwa, H. S. *Appl. Organomet. Chem.* **1991**, *5*, 349.

[9] (a) Desplanches, C.; Ruiz, E.; Alvarez, S. *Eur. J. Inorg. Chem.* **2003**, 1756–1760. (b) Larionova, J.; Mombelli, B.; Sanchiz, J.; Kahn, O. *Inorg. Chem.* **1998**, *37*, 679–684.

[10] (a) Pearson, A. J.; Hwang, J. J. *Tetrahedron Lett.* **2001**, *42*, 3533. (b) Padilla-Tosta, M. E.; Lloris, J. M.; Martínez-Máñez, R.; Pardo, T.; Sancenón, F.; Soto, J.; Marcos, M. D. *Eur. J. Inorg. Chem.* **2001**, 1221–1226.

[11] (a) Aquino, M. A. S. *Coord. Chem. Rev.* **1998**, *170*, 141–202. (b) Bruce, D. W. *J. Chem. Soc., Dalton Trans.* **1993**, 2983. (c) Hudson, S. A.; Maitlis, P. M. *Chem. Rev.* **1993**, *93*, 861–885. (d) Espinet, P.; Esteruelas, M. A.; Oro, L. A.; Serrano, J. L.; Sola, E. *Coord. Chem. Rev.* **1992**, *117*, 215. (e) Giroud-Godquin, A. M.; Maitlis, P. M. *Angew. Chem., Int. Ed. Engl.* **1991**, *30*, 375.

often accompanies the change in the oxidation state of the ruthenium metal. One classical example of electrochemically driven linkage isomerization involving dmso ligands is given by $[Ru(NH_3)_5(dmso)]^{2+}$ (**Figure 1**).[12]



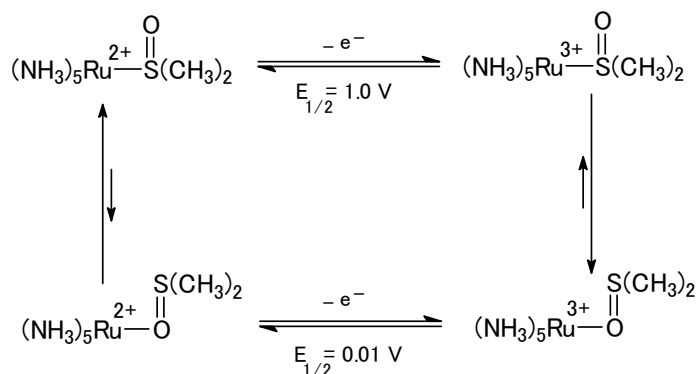**Figure 1.** Redox behavior of $[Ru(NH_3)_5(dmso)]^{2+}$.

In the reduced form, the dmso ligand is coordinated by the S atom, i.e., $[Ru(NH_3)_5(S\text{-}dmso)]^{2+}$, as a consequence of the remarkable $\pi$-backbonding properties of the ruthenium(II) ion. High stabilization of the reduced complex is reflected in its high $E^\circ$ value, i.e., 1.0 V. Oxidation of the complex leads to a $S$-dmso to $O$-dmso linkage isomerization, giving rise to a new wave at 0.01 V, corresponding to the Ru($O$-dmso) (III/II) couple, in cyclic voltammograms. Another remarkable example is given by the asymmetric binuclear (1,5-dithiocyclooctane 1-oxide) bis(pentammineruthenium) complex reported by Sano and Taube (**Figure 2**).[13] They showed that linkage isomerization can lead to molecular hysteresis, a phenomenon that can be used to develop molecular memories and to reach an understanding of memory phenomena in nature.

---

[12] Tomita, A.; Sano, M. *Inorg. Chem.* **1994**, *33*, 5825.

[13] (a) Tomita, A.; Sano, M. *Inorg. Chem.* **2000**, *39*, 200–205. (b) Sano, M.; Taube, H. *Inorg. Chem.* **1994**, *33*, 705–709. (c) Sano, M.; Taube, H. *J. Am. Chem. Soc.* **1991**, *113*, 2327–2328.
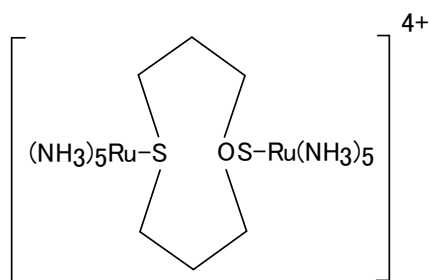
$$[(NH_3)_5Ru\text{-}S \qquad OS\text{-}Ru(NH_3)_5]^{4+}$$

**Figure 2**

Apart from their importance as molecular memory devices, Ru-dmso complexes are interesting as starting materials in the synthesis of new organometallic and coordination compounds[14] and as catalysts for organic transformations. Moreover, particular attention has been paid to their applications in medical chemistry as radiosensitizers[15] and, especially, as antitumoral and antimetastatic agents.[2]
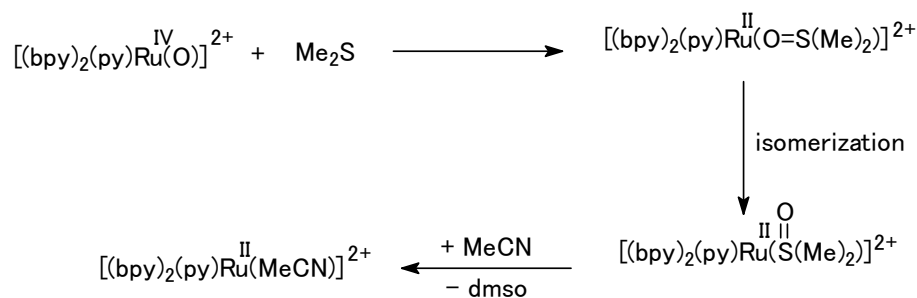
### 1.1.1- Ru-dmso complexes as catalysts.

The ambidentate nature of the dmso ligand has its own implications in the reactivity of Ru-dmso complexes. An example is given in the system described by Roecker *et al.*[16] for the conversion of dimethyl sulfide into dmso by a ruthenium complex (**Scheme 1**). It involves a transient *O*-bonded dmso which is isomerized into the *S*-bonded complex:

---

[14] (a) Alessio, E. *Chem. Rev.* **2004**, *104*, 4203–4242. (b) Crochet, P.; Gimeno, J.; García-Granda, S.; Borge, J. *Organometallics* **2001**, *20*, 4369–4377. (c) Malik, K. Z.; Robinson, S. D.; Steed, J. W. *Polyhedron* **2000**, *19*, 1589–1592. (d) Cingi, M. B.; Lanfranchi, M.; Pellinghelli, M. A.; Tegoni, M. *Eur. J. Inorg. Chem.* **2000**, 703–711. (e) Hesek, D.; Inoue, Y.; Everitt, S. R. L.; Ishida, H.; Kunieda, M.; Drew, M. G. B. *Chem. Comm.* **1999**, 403–404. (f) Yamamoto, Y.; Sugawara, K.-I.; Aiko, T.; Ma, J.-F. *J. Chem. Soc., Dalton Trans.* **1999**, 4003–4008. (g) Alessio, E.; Macchi, M.; Heath, S. L.; Marzilli, L. G. *Inorg. Chem.* **1997**, *36*, 5614–5623. (h) Davies, J. A. *Adv. Inorg. Chem. Radiochem.* **1981**, *24*, 115.

[15] (a) Mandal, P. C. *J. Electroanal. Chem.* **2004**, *570*, 55–61. (b) Skov, K. A.; Farrell, N. P. *Int. J. Radiat. Biol.* **1990**, *57*, 947–958. (c) Chan, P. K. I.; James, B. R.; Frost, D. C.; Chan, P. K. H.; Hu, H.-L. *Can. J. Chem.* **1989**, *67*, 508. (d) Chan, P. K.; Skov, K. A.; James, B. R. *Int. J. Radiat. Biol.* **1987**, *52*, 49–55. (e) Chan, P. K.; Skov, K. A.; James, B. R.; Farrell, N. P. *Int. J. Radiat. Oncol. Biol. Phys.* **1986**, *12*, 1059–1062.

[16] Roecker, L.; Dobson, J. C.; Vining, W. J.; Meyer, T. J. *Inorg. Chem.* **1987**, *26*, 779–781.

$$[(bpy)_2(py)Ru^{IV}(O)]^{2+} + Me_2S \longrightarrow [(bpy)_2(py)Ru^{II}(O=S(Me)_2)]^{2+}$$

isomerization

$$[(bpy)_2(py)Ru^{II}(MeCN)]^{2+} \xleftarrow[-\ dmso]{+\ MeCN} [(bpy)_2(py)Ru^{II}(\overset{O}{\overset{\|}{S}}(Me)_2)]^{2+}$$

**Scheme 1**

Many examples of Ru–dmso complexes acting as catalysts have been reported so far. Several significant examples are next detailed:

– Ruthenium(II) complexes of the type $RuX_2(dmso)_4$ (X = Cl, Br, SnCl$_3$, SCN) can function as good catalysts for the selective oxygen oxidation of sulfides to sulfoxides in alcoholic solvents.[17] [(dmso)$_2$H][*trans*–RuCl$_4$(dmso)$_2$], *mer*–[RuCl$_3$(dmso)$_3$], *mer*–[RuCl$_3$(dmso)$_2$(MePhSMe)], and *mer*–[RuCl$_3$(dmso)(MePhSMe)$_2$] are also efficient catalysts for this reaction under mild conditions.[18]

– RuCl$_2$(dmso)$_4$ has also been found to be an active catalyst precursor for 1–hexene hydrogenation in water/organic solvent biphasic systems, reaching 98% total conversion (400 psi H$_2$, 80 °C, 6 h), with *n*–hexane as the principal product.[19] Recently, RuCl$_2$(tppms)$_3$(dmso) (tppms = triphenylphosphine monosulfonate) has been found to catalyze 1–hexene hydrogenation (500 psi H$_2$ and 100°C) in a two–phase system, with 80% conversion in 24 h, with little substrate isomerization. This complex shows good stability and can be reused several times with little activity loss.[20]

– The complex *mer*–[RuCl$_3$(dmso)(phen)] and the analogous complex *cis,cis*–[RuCl$_2$(dmso)$_2$(phen)] exhibit high catalytic activity in the isomerization of 3–buten–2–ol

[17] (a) Riley, D. P.; Oliver, J. D. *Inorg. Chem.* **1986**, *25*, 1814–1821. (b) Riley, D. P. *Inorg. Chem.* **1983**, *22*, 1965.

[18] Srivastava, R. S.; Milani, B.; Alessio, E.; Mestroni, G. *Inorg. Chim. Acta* **1992**, *191*, 15–17.

[19] Fontal, B.; Anzelotti, A.; Reyes, M.; Bellandi, F.; Suarez, T. *Catal. Lett.* **1999**, *59*, 187–190.

[20] Suárez, T.; Fontal, B.; Reyes, M.; Bellandi, F.; Contreras, R. R.; Ortega, J. M.; León, G.; Cancines, P.; Castillo, B. *React. Kinet. Catal. Lett.* **2004**, *82*, 325–331.

to butanone.[21]

–   The ruthenium(II) catalysts $[Ru(H_2O)_2(dmso)_4](BF_4)_2$, $[RuCl_2(dmso)_4]$, and [RuPcS] (PcS = tetra–sulfo–phthalocyaninate) are effective catalysts for the oxidation of chlorinated organics (polychlorobenzenes, polychlorophenols and chloro–, bromo–, iodo– and nitro–benzene) in the presence of hydrogen peroxide or mono–persulfate at room temperature, yielding mainly to hydrochloric acid and carbon dioxide.[22]

–   Some ruthenium complexes, $[Ru^{II}(babp)(dmso)(L)]$, being $H_2babp$ = 6,6'–bis(benzoylamino)–2,2'–bipyridine and L = dmso, imidazole, or pyridine derivatives, have been proven to be active as catalysts for the epoxidation of unfunctionalized olefins in the presence of iodosobenzene.[23] Ruthenium bis(bipyridine) sulfoxide complexes also exhibit high catalytic activity for this reaction using [bis(acetoxy)iodo]benzene as oxidant.[24]

–   $fac$–[RuCl_2(dmso)(N,P,N)] where N,P,N = bis(2–oxazolin–2–ylmethyl)phenylphospine catalyzes the transfer hydrogenation reaction between 2–propanol and ketones (cyclohexanone and acetophenone).[25] Hydrogenation of acetophenone in 2–propanol has also been reported using $trans$–[RuCl_2($\kappa^2$–P,N–2–Ph_2PC_6H_4CH=N^tBu)(dmso)_2] and [RuCl_2($\kappa^2$–P,N–2–Ph_2PC_6H_4CH_2NH^tBu)(dmso)] as catalysts.[14b]

## 1.1.2– <u>Ru–dmso complexes as anticancer agents.</u>

Cancer is one of the major causes of death in the western world. Current treatment of cancer is limited to surgery, radiotherapy, and the use of cytotoxic agents, despite their well known side effects and problems associated with the development of resistance. For

[21] Van der Drift, R. C.; Sprengers, J. W.; Bouwman, E.; Mul, W. P.; Kooijman, H.; Spek, A. L.; Drent, E. *Eur. J. Inorg. Chem.* **2002**, 2147–2155.

[22] Bressan, M.; d'Alessandro, N.; Liberatore, L.; Morvillo, A. *Coord. Chem. Rev.* **1999**, *185–186*, 385–402.

[23] Jitsukawa, K.; Shiozaki, H.; Masuda, H. *Tetrahedron Lett.* **2002**, *43*, 1491–1494.

[24] Pezet, F.; Aithaddou, H.; Daran, J. C.; Sasaki, I.; Balavoine, G. G. *Chem. Comm.* **2002**, *5*, 510–511.

[25] Braunstein, P.; Fryzuk, M. D.; Naud, F.; Rettig, S. J. *J. Chem. Soc., Dalton Trans.* **1999**, 589–594.

most forms of disseminated cancer, however, no curative therapy is available, and the discovery and development of novel active chemotherapeutic agents is largely needed.

*Cisplatin*, or *cis*-diamminedichloroplatinum(II) (**Figure 3**) is an anticancer agent that has been in use for over 30 years. Its use is widespread and few other anticancer agents have been proven as effective as it. However, serious side effects limit its clinical use. Another major clinical problem is tumor resistance, which can be either intrinsic or acquired. The limitations of *cisplatin* have stimulated the search for alternative metal-based anticancer agents and alternative pharmaceutical formulations of platinum, with more acceptable toxicity profiles, but retention, and if possible expansion, of efficacy.
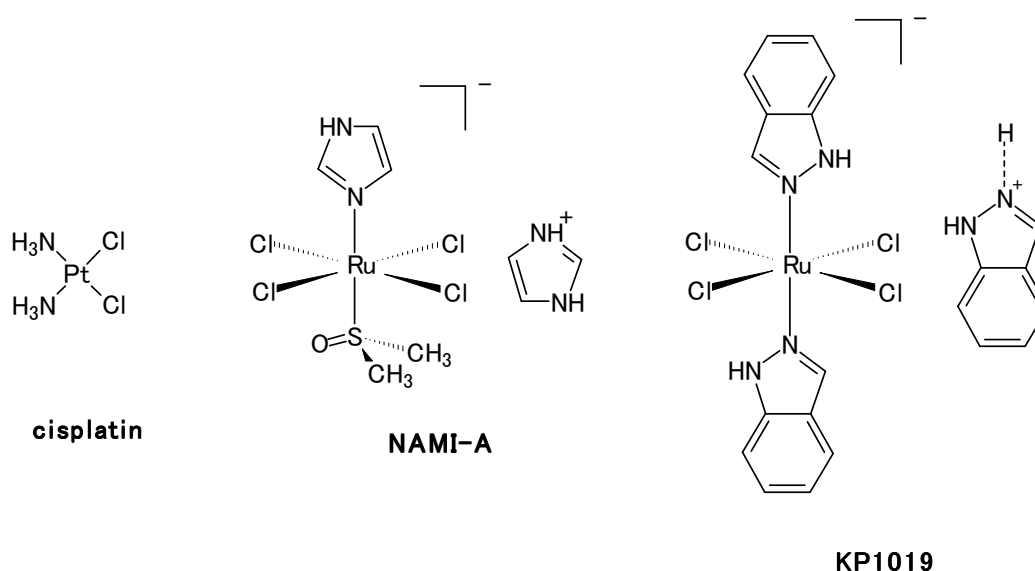


**Figure 3.** Structure of complexes with anticancer activity.

Several Ru$^{II}$ and Ru$^{III}$ complexes with coordinated dimethyl sulfoxide have been shown to possess good antitumor and, above all, antimetastatic properties against animal models. Among these compounds, a Ru$^{III}$ complex called NAMI-A, [ImH][*trans*-RuCl$_4$(*S*-dmso)(Im)] (Im = imidazole) (**Figure 3**), was selected because of its very good antimetastatic activity and on October 1999 it was introduced into phase I clinical trials at the Netherland Cancer Institute of Amsterdam.[2f,26] NAMI-A is one of the very few non-platinum antitumor

[26] (a) Ravera, M.; Baracco, S.; Cassino, C.; Colangelo, D.; Bagni, G.; Sava, G.; Osella, D. *J. Inorg. Biochem.* **2004**, *98*, 984–990. (b) Bacac, M.; Hotze, A. C. G.; Van der Schilden, K.; Haasnoot, J. G.; Pacor, S.; Alessio, E.;

drugs, and the first ruthenium-based compound, to reach clinical phase trials. This compound has already accomplished phase I clinical trials and will hopefully enter phase II soon.

Several NAMI-A-type monomeric and dimeric Ru(III) complexes have been recently developed.[27] In such compounds, the coordinative environment of each Ru(III) nucleus is very similar to that of NAMI-A. Preliminary in vivo results have showed that some of them have an antimetastatic activity comparable to that of NAMI-A at dosages that are 3.5 times lower in terms of moles of Ru.

Another ruthenium compound, [indH][*trans*-RuCl$_4$(ind)$_2$] (ind = indazole), also reached phase I trials at the end of 2003. This complex, developed by Bernhard Keppler and termed KP1019 (see **Figure 3**), proved to be active against platinum-resistant colorectal tumors.[28]

## 1.2- Properties of the Ru-polypyridyl complexes with aqua ligands.

Ruthenium polypyridyl aqua complexes have proven to be very suitable in the design of redox catalysts for a variety of reasons. First, these compounds are useful catalysts in redox reactions since one or more oxidation states are frequently available, thus enabling multiple electron transfers to occur. In addition, their substitutionally inert nature allows for chemically reversible electron transfer uncomplicated by ligand exchange. Therefore,
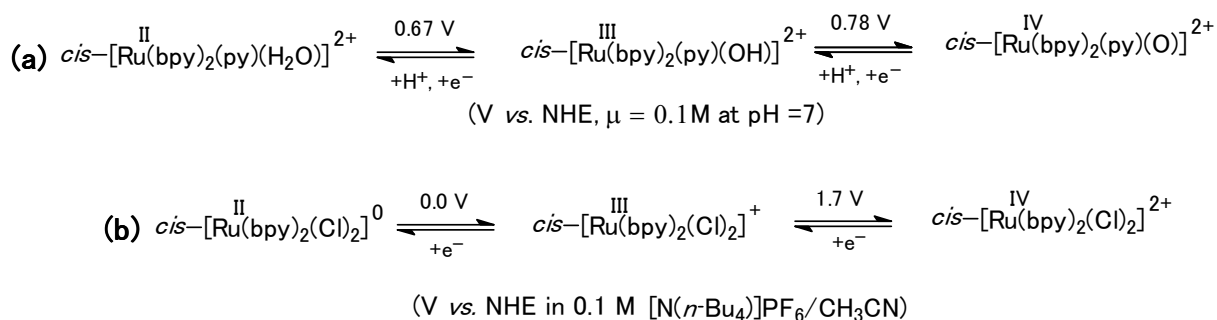
Sava, G.; Reedijk, J. *J. Inorg. Biochem.* **2004**, *98*, 402–412. (c) Alessio, E.; Mestroni, G.; Bergamo, A.; Sava, G. *Curr. Topics Med. Chem.* **2004**, *4*, 1525–1535. (d) Sava, G.; Pacor, S.; Mestroni, G.; Alessio, E. *Anticanc. Drugs* **1992**, *3*, 25.

[27] (a) Velders, A. H.; Bergamo, A.; Alessio, E.; Zangrando, E.; Haasnoot, J. G.; Casarsa, C.; Cocchietto, M.; Zorzet, S.; Sava, G. *J. Med. Chem.* **2004**, *47*, 1110–1121. (b) Serli, B.; Iengo, E.; Gianferrara, T.; Zangrando, E.; Alessio, E. *Metal-Based Drugs* **2001**, *8*, 9–18. (c) Alessio, E.; Iengo, E.; Zorzet, S.; Bergamo, A.; Coluccia, M.; Boccarelli, A.; Sava, G. *J. Inorg. Biochem.* **2000**, *79*, 173–177. (d) Iengo, E.; Mestroni, G.; Geremia, S.; Calligaris, M.; Alessio, E. *J. Chem. Soc., Dalton Trans.* **1999**, 3361–3371.

[28] (a) Pongratz, M.; Schluga, P.; Jakupec, M. A.; Arion, V. B.; Hartinger, C. G.; Allmaier, G.; Keppler, B. K. *J. Anal. At. Spectrom.* **2004**, *19*, 46–51. (b) Piccioli, F.; Sabatini, S.; Messori, L.; Orioli, P.; Hartinger, C. G.; Keppler, B. K. *J. Inorg. Biochem.* **2004**, *98*, 1135–1142. (c) Galanski, M.; Arion, V. B.; Jakupec, M. A.; Keppler, B. K. *Curr. Pharm. Des.* **2003**, *9*, 2078–2089. (d) Keppler, B. K.; Henn, M.; Juhl, U. M.; Berger, M. R.; Niebl, R.; Wagner, F. E. *Prog. Clin. Biochem. Med.* **1989**, *10*, 41–69.

these ruthenium complexes tend to retain their integrity in solution and are relatively easy to study. Finally, the oxo-aqua ligands provide for rapid proton transfer concomitant with electron transfer, permitting the accessibility of several oxidation states via gain or loss of protons.

The example shown in **Scheme 2** is typical for ruthenium complexes with an aqua ligand. Oxidation of the Ru metal center increases the acidity of the bound Ru-O-H protons, which accounts for the pH-dependent redox behavior of this kind of compounds. As suggested in **Scheme 2a**, both, the potentials of the Ru(III/II) and Ru(IV/III) couples have a complex pH dependence. If we compare the redox potential values for the aqua complex and the chloro complex $cis$-[$Ru^{II}$(bpy)$_2$(Cl)$_2$] in **Scheme 2b**, a difference is remarkable; whereas for the chloro complex the difference between the Ru(IV/III) and Ru(III/II) couples is 1.7 V, for the aqua complex this difference is only 0.11 V.

**(a)** $cis$-[$\overset{II}{Ru}$(bpy)$_2$(py)(H$_2$O)]$^{2+}$  $\underset{+H^+, +e^-}{\xrightarrow{0.67\ V}}$  $cis$-[$\overset{III}{Ru}$(bpy)$_2$(py)(OH)]$^{2+}$  $\underset{+H^+, +e^-}{\xrightarrow{0.78\ V}}$  $cis$-[$\overset{IV}{Ru}$(bpy)$_2$(py)(O)]$^{2+}$

(V $vs.$ NHE, $\mu = 0.1$ M at pH =7)

**(b)** $cis$-[$\overset{II}{Ru}$(bpy)$_2$(Cl)$_2$]$^{0}$  $\underset{+e^-}{\xrightarrow{0.0\ V}}$  $cis$-[$\overset{III}{Ru}$(bpy)$_2$(Cl)$_2$]$^{+}$  $\underset{+e^-}{\xrightarrow{1.7\ V}}$  $cis$-[$\overset{IV}{Ru}$(bpy)$_2$(Cl)$_2$]$^{2+}$

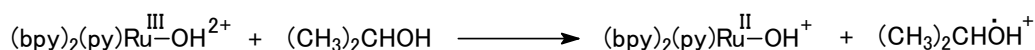(V $vs.$ NHE in 0.1 M [N($n$-Bu$_4$)]PF$_6$/CH$_3$CN)

**Scheme 2**

These data point to a dramatic stabilization of $Ru^{IV}$ in the aqua-containing coordination environment. This is caused by proton loss and electronic stabilization of the higher oxidation state by oxo formation, which causes the near overlap of Ru(IV/III) and Ru(III/II) couples.[29] There is an important implication for reactivity in this near overlap. Thermodynamically, $Ru^{IV}$ is nearly as good acting as a two-electron oxidant as a one-electron oxidant at pH = 7. This fact has very important implications in catalysis since two-electron pathways with concomitant formation of the two-electron oxidized product

---

[29] Che, C. M.; Yam, V. W. W. *Adv. Inorg. Chem.* **1992**, *39*, 233.
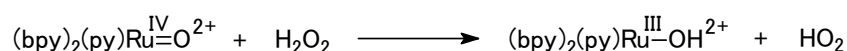
are the most favorable energetically. An additional advantage is that two-electron pathways avoid high energy one-electron intermediates which have often indiscriminate chemistries that can lead to a lack of selectivity.[30] The oxo group is also mechanistically important since it provides an O transfer pathway, and initial lead-in site for attack on a substrate, or an acceptor site for a transferred hydrogen in a hydride transfer.

Ruthenium-oxo and hydroxo species, generated through the reaction of low-valent ruthenium aqua complexes and various oxidants, are used extensively for the oxidation of organic substrates. These complexes are versatile oxidants, able to provide a variety of redox pathways which are illustrated next with examples:
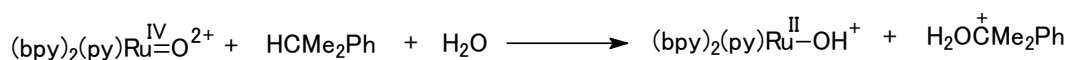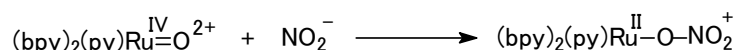
♣ Outer sphere electron transfer:

$$(bpy)_2(py)Ru^{III}\text{-}OH^{2+} + (CH_3)_2CHOH \longrightarrow (bpy)_2(py)Ru^{II}\text{-}OH^+ + (CH_3)_2C\dot{H}\dot{O}H^+$$

♣ Proton-coupled electron transfer:

$$(bpy)_2(py)Ru^{IV}\text{=}O^{2+} + H_2O_2 \longrightarrow (bpy)_2(py)Ru^{III}\text{-}OH^{2+} + HO_2$$

♣ Hydride transfer:

$$(bpy)_2(py)Ru^{IV}\text{=}O^{2+} + (CH_3)_2CHOH \longrightarrow (bpy)_2(py)Ru^{II}\text{-}OH^+ + (CH_3)_2C\text{=}OH^+$$

♣ Hydride transfer and nucleophilic addition:

$$(bpy)_2(py)Ru^{IV}\text{=}O^{2+} + HCMe_2Ph + H_2O \longrightarrow (bpy)_2(py)Ru^{II}\text{-}OH^+ + H_2O\overset{+}{C}Me_2Ph$$

♣ Oxygen-atom transfer:

$$(bpy)_2(py)Ru^{IV}\text{=}O^{2+} + NO_2^- \longrightarrow (bpy)_2(py)Ru^{II}\text{-}O\text{-}NO_2^+$$

---

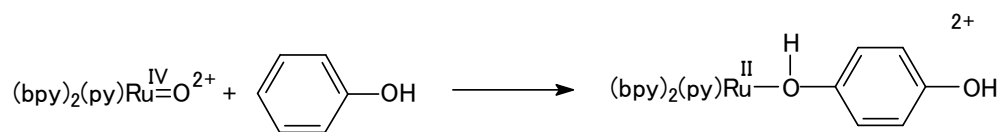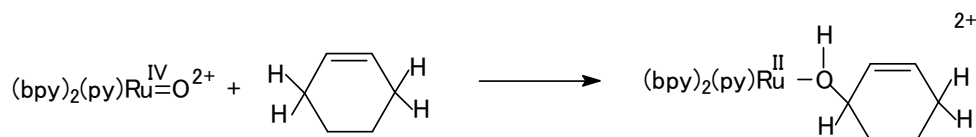[30] (a) Keene, F. R. *Coord. Chem. Rev.* **1999**, *187*, 121. (b) Meyer, T. J. *J. Electrochem. Soc.* **1984**, *131*, 221C.
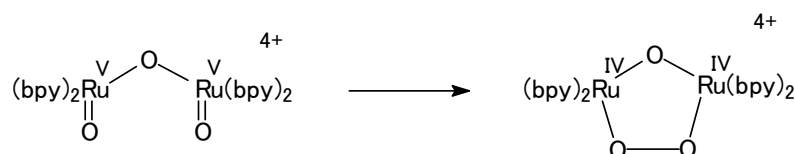
♣ Electrophilic ring attack:



♣ C–H insertion:



♣ Oxidative coupling:



Special attention has been paid to Ru–oxo complexes as catalysts for water oxidation to oxygen. As can be seen in **Equation 1**, the mechanistic demands inherent in $O_2$–evolving from water are the loss of $4e^-$ and $4H^+$ with the formation of an O–O bond. A mechanism involving one–electron transfers is accessible but demands powerful oxidants, since intermediates such as the hydroxyl radical, $\cdot OH$, or $\cdot OH_2^+$ are of high energy thermodynamically.

$$2H_2O \longrightarrow O_2 + 4H^+ + 4e^- \qquad (E° = -1.23 \text{ V } vs. \text{ NHE})$$
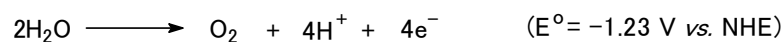
**Equation 1**

One possible approach to the design of a water oxidation catalyst is a dimeric structure with two Ru–oxo groups in close proximity. A paradigmatic example is the *blue dimer* reported by Meyer *et al.* in 1982,[31] which is the first reported ruthenium catalyst able to

[31] (a) Gilbert, J. A.; Eggleston, D. S.; Murphy, W. R.; Geselowitz, D. A.; Gersten, S. W.; Hodgson, D. J.; Meyer, T. J. *J. Am. Chem. Soc.* **1985**, *107*, 3855–3864. (b) Gersten, S. W.; Samuels, G. J.; Meyer, T. J. *J. Am. Chem.*
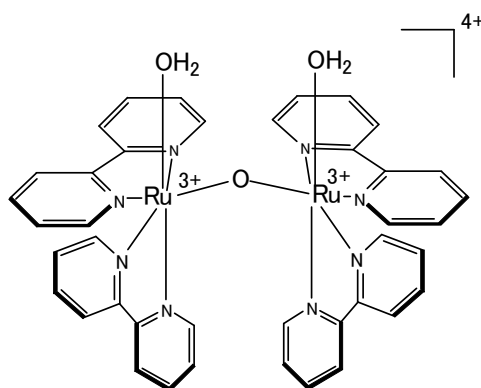
oxidize water to molecular oxygen (**Figure 4**).



**Figure 4.** The *blue dimer* reported by Meyer and coworkers.[31]

In the next section, an overview to natural and artificial photosynthesis is given, with special emphasis to the existing water oxidation catalysts and their mechanism of action.

*Soc.* **1982**, *104*, 4029.

## 2- An introduction to photosynthesis and water oxidation catalysis.

In today's society there is an increasing demand for energy. This need is to a large extent supplied by the use of fossils fuels. However, the supply of fossils fuels will be used up in the near future and they are not, therefore, a long-term solution for the increasing need for energy. If other resources could be used as a source of energy, that would allow us to use fossil fuels in a more sustainable way to produce common products such as detergents, synthetic fibers, plastics, paints, food additives, pesticides, etc. Another, even more important reason why the use of fossils fuels should be avoided, is their negative effect on the environment. Thus, the need to find alternative, renewable and environmental friendly energy sources is becoming more and more pressing. The amount of solar energy that reaches the Earth's surface in one hour is equal to the amount of fossil fuels that is consumed globally in one year.[32] If this enormous energy could be used to produce a clean and renewable energy source, the advantages would be obvious.

In photosynthesis, green plants convert solar energy into chemical energy that they need for their survival. The idea of constructing an artificial device capable of converting sunlight into electricity or some kind of fuel, by mimicking the processes responsible for the energy conversion in photosynthesis, is a major driving force in artificial photosynthesis. These kinds of devices are also attractive from an environmental viewpoint, since they would not generate any harmful byproducts.

During the last 30 years, much effort has been devoted to the construction of an artificial system that mimics the natural way of converting solar energy to chemical energy. By using knowledge obtained from the natural system, several model systems have been constructed and studied. These model systems can mainly be divided into two categories: those with a photosensitizer linked to electron donors and acceptors mimicking the

---

[32] Freemantle, M. *Chem. Eng. News* **1998**, *76*, 37-46.

primary charge-separation processes,[33] and those mimicking the manganese complex of PSII. The former systems include mimics of the acceptor side of the reaction centers PSI and PSII,[34] but have only rarely involved the transfer of more than one electron or been coupled to any molecular catalyst.[34a,35] The artificial mimics of the manganese complex, on the other hand, have often been only structural mimics, with only a few examples is of multi-step oxidation or verified catalytic activity.

In the present chapter, we briefly review the essentials of the PSII donor side, and point out a few recent results for manganese and ruthenium compounds that are of particular importance due to their ability to catalyze water oxidation.

## 2.1- Natural photosynthesis.

In natural photosynthesis, light is converted into chemical energy through a chain of electron transfer reactions. In the oxygenic photosynthesis of plants, algae and cyanobacteria, two photosynthetic reaction centers, Photosystems I and II, work in series according to the so-called Z-scheme. Each of the two reaction centers is a large, membrane-spanning protein complex that separates charge across the membrane when excited by light. In Photosystem II (PSII) (**Figure 5**), the photo-excited chlorophylls of the primary electron donor $P_{680}$ are oxidized by electron transfer to the quinones on the acceptor side of the reaction center. In a subsequent reaction, $P_{680}$ is regenerated by electron transfer from a tetranuclear manganese complex on the donor side, via a tyrosine residue. Thus, each photon that is absorbed leads as a whole to the transfer of one electron from the manganese complex to the secondary quinone acceptor, $Q_B$, which is a

---

[33] (a) Kurreck, H.; Huber, M. *Angew. Chem., Int. Ed. Engl.* **1995**, *34*, 849–866. (b) Sauvage, J. P.; Collin, J. P.; Chambron, J. C.; Guillerez, S.; Coudret, C.; Balzani, V.; Barigelletti, F.; DeCola, L.; Flamigni, L. *Chem Rev.* **1994**, *94*, 993–1019. (c) Gust, D.; Moore, T. A.; Moore, A. L. *Acc. Chem. Res.* **1993**, *26*, 198–205. (d) Wasielewski, M. R. *Chem. Rev.* **1992**, *92*, 435–461.

[34] (a) Steinberg-Yfrach, G.; Rigaud, J.-L.; Durantini, E. N.; Moore, A. L.; Gust, D.; Moore, T. A. *Nature* **1998**, *392*, 479. (b) Osuka, A.; Nakajima, S.; Okada, T.; Taniguchi, S.; Nozaki, K.; Ohno, T.; Yamazaki, I.; Nishimura, Y.; Mataga, N. *Angew. Chem., Int. Ed. Engl.* **1996**, *35*, 92–95. (c) Hasharoni, K.; Levanon, H.; Greenfield, S. R.; Gosz-tola, D. J.; Svec, W. A.; Wasielewski, M. R. *J. Am. Chem. Soc.* **1995**, *117*, 8055–8056.

loosely bound plastoquinone molecule. When a second photon is absorbed, $Q_B$ becomes doubly reduced and then takes up two protons to form the neutral hydroquinone species $QH_2$, which is mobile and is exchanged for a new plastoquinone (Q) from the membrane-associated quinone pool.
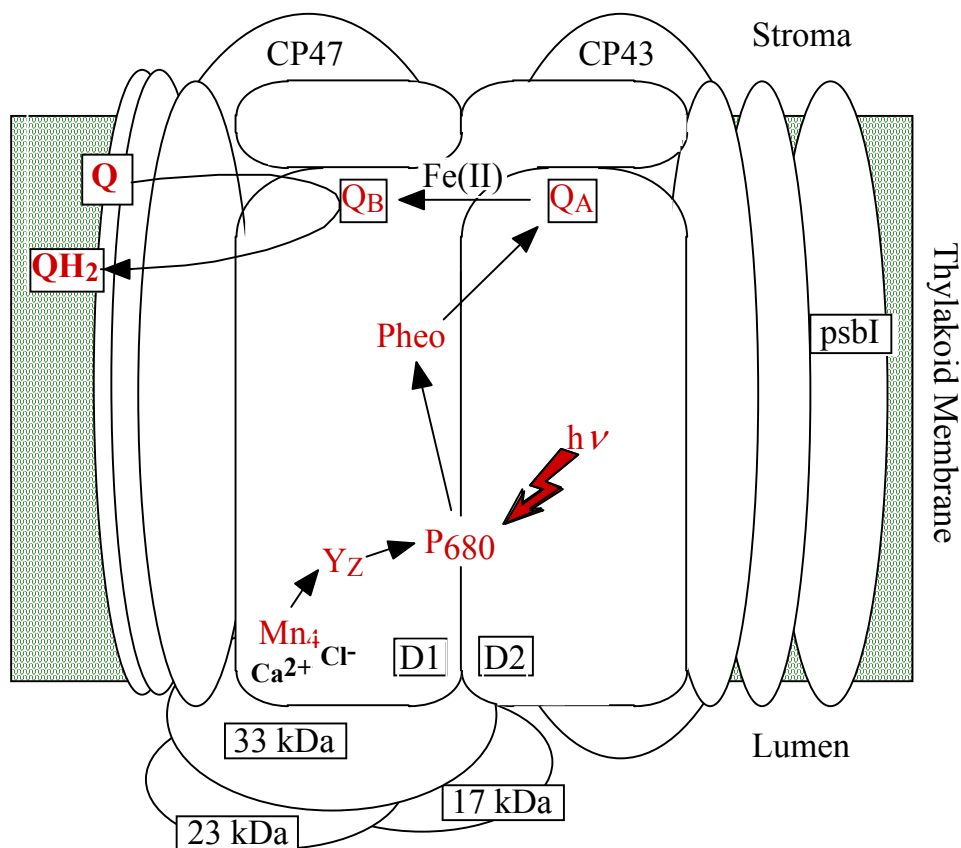


**Figure 5.** The primary electron transfer pathway (black arrows) in photosystem II. Abbreviations: $Mn_4$, the manganese tetramer; $Y_Z$, the redox-active tyrosine of D1 subunit; $P_{680}$, the primary electron donor of photosystem II; Pheo, pheophytin; $Q_A$, membrane-bound plastoquinone; $Q_B$, exchangeable plastoquinone.

In subsequent reactions, the $QH_2$ delivers two electrons to Photosystem I via several electron carriers, where they are used as the substrate in another sequence of light-induced electron transfers leading to the reduction of NADP, and eventually to $CO_2$-fixation (**Figure 6**, right).

---

[35] Molnar, S. M.; Nallas, G.; Bridgewater, J. S.; Brewer, K. J. *J. Am. Chem. Soc.* **1994**, *116*, 5206.

Reduction Potential (V)

-1.2

0.8

-0.4

0.0

0.4

0.8

1.2

P680*

Pheo

QA

hν

QB

H₂O

Mn₄

O₂

Yz

P680

Photosystem II

cyt *b6/f* complex

P700*

A0

A1

Fx

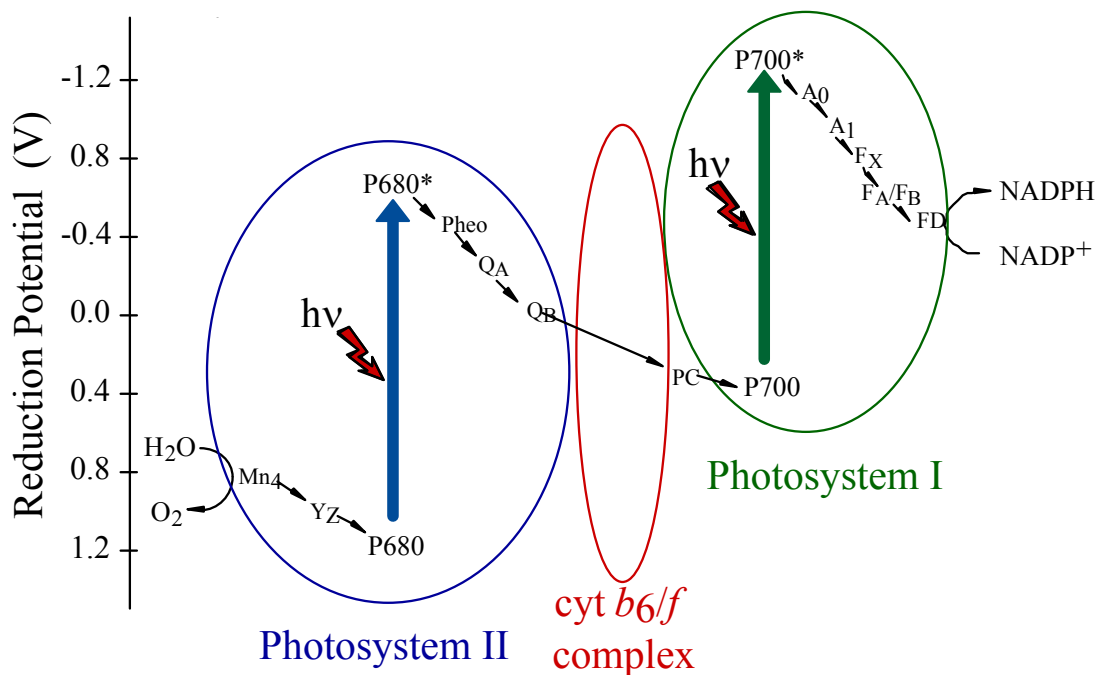FA/FB

FD

NADPH

NADP⁺

hν

PC

P700

Photosystem I

**Figure 6.** The Z–scheme of photosynthesis.[36] Black arrows represent the direction of electron transfer; the blue and green arrows represent the two independent photoexcitations in PSII and PSI, respectively. Abbreviations: $Mn_4$, the manganese tetramer; Yz, redox–active tyrosine; $P_{680}$ and $P_{680*}$, the chlorophyll special pair of PSII and its excited state; Pheo, pheophytin; $Q_A$, membrane–bound plastoquinone; $Q_B$, exchangeable plastoquinone; PC, plastocyanin; $P_{700}$ and $P_{700*}$, the chlorophyll special pair of PSI and its excited state; $A_0$, chlorophyll *a* molecule; $A_1$, phylloquinone (vitamin K) molecule; $F_X/F_A/F_B$, iron–sulfur protein centers; FD, ferredoxin; NADPH, reduced form of nicotinamide adenine dinucleotide phosphate.

In PSII (**Figure 6**, left) the electrons are provided by water that is oxidized to molecular oxygen. Water is abundant, which gives the oxygenic organisms an advantage over photosynthetic species that use other electron substrates. However, in order to oxidize water at reasonably low potentials, without forming high–energy intermediates, four electrons have to be taken in one step (**Equation 1**).

Water oxidation in PSII is catalyzed by the tetranuclear manganese complex on the donor

[36] Hill, R.; Bendall, F. *Nature* **1960**, *186*, 136–137.

side.[37] During the light-induced charge separation cycles, this complex serves to accumulate the oxidizing equivalents needed for the reaction shown in **Equation 1**. This is highly demanding, as it has to couple the one-electron light-induced reactions to the four-electron water oxidation. Thus, each oxidation state is stable on the time scale of seconds to minutes, which is sufficiently long for the next photon to arrive.

After four consecutive steps of light excitation and oxidation, the water oxidation cycle is completed; molecular oxygen is released and new water molecules bind to the complex, which reverts to its most reduced state.

## 2.2- The oxygen-evolving complex (OEC).

The manganese cluster is the catalytic center of the water splitting enzyme in natural photosynthesis. Together with the part of the PSII protein complex directly involved in the water splitting, it is denoted the *oxygen-evolving complex* (OEC). The cluster consists of four manganese ions and oxygen atoms that serve as a charge accumulator. The positive charge from the photoinduced charge separation process is used to extract electrons from water with the result that water is oxidized to oxygen and protons in a four-electron process.

The cluster passes through several oxidation states during this multi-electron redox process. Successively absorbed photons drive the cycle of the OEC through four semistable states: $S_1$ (dark stable state) $\rightarrow S_2 \rightarrow S_3 \rightarrow S_4 \rightarrow S_0 \rightarrow S_1$ (Kok cycle,[38] **Figure 7**) The $S_3$–$S_0$ transition is assumed to involve the formation of a transient intermediate state, the $S_4$; the $S_4$–$S_0$ transition is coupled to the release of molecular oxygen.[39]

---

[37] (a) Yagi, M.; Kaneko M. *Chem. Rev.* **2001**, *101*, 21. (b) Nugent, J. (Ed.) Photosynthetic water oxidation, Special issue of *Biochim. Biophys. Acta* **2001**, *1503*, 1–253. (c) Rüttinger, W.; Dismukes, G. C. *Chem. Rev.* **1997**, 1. (d) Yachandra, V. K.; Sauer, K.; Klein, M. P. *Chem. Rev.* **1996**, *96*, 2927. (e) Debus, R. J. *Biochim. Biophys. Acta* **1992**, *1102*, 269.

[38] Kok, B.; Forbush, B.; McGloin, M. *Photochem. Photobiol.* **1970**, *11*, 457.

[39] Iuzzolino, L.; Dittmer, J.; Dorner, W.; Meyer-Klauche, W.; Dau, H. *Biochemistry* **1998**, *37*, 17112–17119.
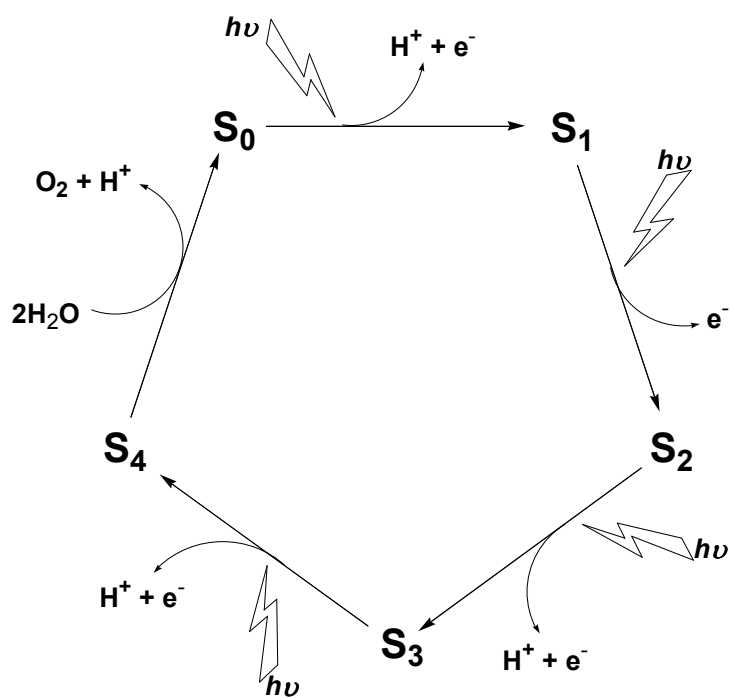
**Figure 7.** The Kok S-state cycle.

A lack of knowledge of the intimate mechanism of the catalytic process that leads to oxygen production has hindered the design of multi-electron redox catalysts for artificial photosynthesis. However, the OEC is currently the subject of intensive research and recently, important advances on the structure of PSII with the manganese cluster have been reported by Ferreira *et al.*[40] From a crystal structure at 3.5 Å resolution, the authors conclude that the OEC is a cubane-like $Mn_3CaO_4$ cluster with a mono-μ-oxo bridge to a fourth Mn ion (**Figure 8**). On the basis of this proposed structure, they discuss the possible mechanism of the oxygen-evolving reaction.

[40] Ferreira, K. N.; Iverson, T. M.; Maghlaoui, K.; Barber, J.; Iwata, S. *Science* **2004**, *303*, 1831–1838.
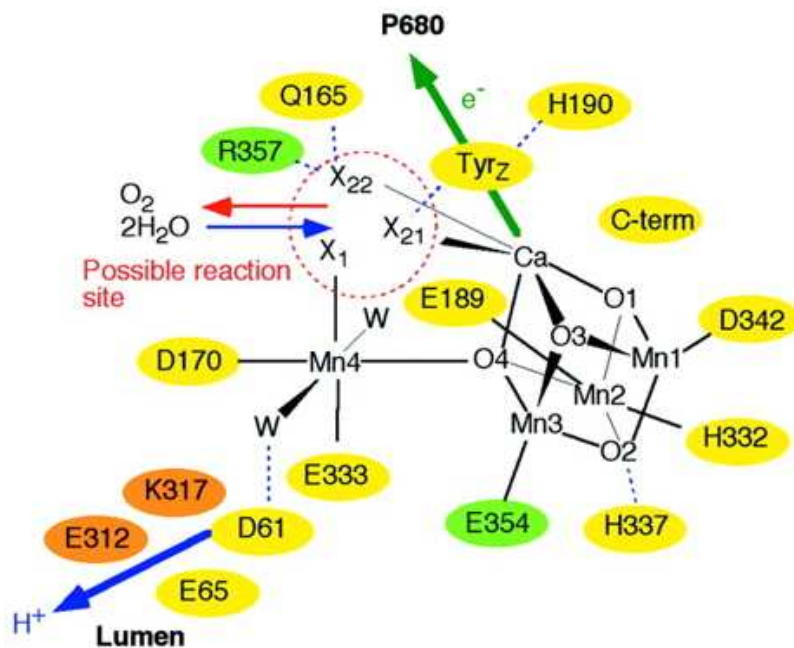
**Figure 8.** Schematic view of the OEC. Residues in D1, D2 and CP43 subunits are shown in yellow, orange and green, respectively. $X_1$, $X_{21}$ and $X_{22}$ are possible substrate water binding positions to Mn4 ($X_1$) and to $Ca^{2+}$ ($X_{21}$ and $X_{22}$). Possible water molecules are indicated as W. Possible hydrogen bonds are shown as light-blue dotted lines.

## 2.3- Artificial photosynthesis. Functional model systems for the OEC.

A large number of model compounds has been synthesized which provide valuable insights about the structural and electronic characteristics of the manganese tetramer of the OEC. The mimicking of the water oxidation using inorganic compounds, however, has been largely unsuccessful. So far, only a handful of heterogeneous and homogeneous water oxidation systems has been identified. Although the reactants and catalysts of these systems are significantly different from those of the biological system, the study of these catalyses helps the understanding of the structural and chemical properties of the key intermediates required for water oxidation and thus, aids to our understanding of the reactions carried out in the OEC. In this section, we will discuss a few examples of close relevance to the water oxidation in PSII.

### 2.3.1- <u>Heterogeneous water oxidation catalysts.</u>

Using photogenerated Ru(bpy)$_3^{3+}$ as oxidant, Shilov *et al.* observed O$_2$-evolving from the mixture of MnO$_2$ and Mn$^{IV}$ pyrophosphate, with the latter compound acting as a sacrificial electron acceptor.[41] Incorporation of Mn$^{IV}$ into phospholipid membranes releases O$_2$ under similar reaction conditions.[42] A Mn$^{V}$ species was proposed to be the key intermediate in both reactions.

Suspensions of the complexes [Mn$_2^{III,IV}$($\mu$–O)$_2$L$_4$](ClO$_4$)$_3$ (L = bpy, **1a**, or phen, **1b**) in water were shown to catalyze heterogeneous water oxidation in the presence of an excess of Ce$^{IV}$.[43] The O$_2$ yields were reported to be independent of pH, even at high pH conditions where Ce$^{IV}$ is known to be unstable. Complex **1a** was found to be more active than **1b** as catalyst, which was attributed to the lower reduction potential of **1a**.[43b] In a similar report using Ce$^{IV}$ as oxidant, [Mn$^{III}$(salen)(H$_2$O)]$^+$ (salen = N,N'–bis(salicylidene)ethylenediamine dianion), either as a suspension of the oxidized complex  or in an adsorbed state onto Kaolin clay, was found to catalyze the oxidation of water and of the NH$_4^+$ ions from (NH$_4$)$_2$[Ce$^{IV}$(NO$_3$)$_6$] to O$_2$ and N$_2$, respectively.[44] The overall turnover number of the catalyst for O$_2$/N$_2$ evolution was 13 and 10 for the suspended and adsorbed catalyst, respectively.

More recently, Yagi and Narita reported a heterogeneously catalyzed O$_2$ evolution, with Ce$^{IV}$ as oxidant (pH = 1) and with [Mn$_2^{III,IV}$O$_2$(trpy)$_2$(OH$_2$)$_2$]$^{3+}$ (**2**) adsorbed on Kaolin clay as catalyst for water oxidation.[45] Under the same conditions, no activity was found for manganese oxides (MnO$_2$ or Mn$_2$O$_3$), Mn$^{2+}$, Mn$^{3+}$ or MnO$_4^-$ ions in solution, or adsorbed Mn$^{2+}$, Mn$^{3+}$ or trpyH$_n^{n+}$ on Kaolin clay. When clay-adsorbed [Mn$_2^{III,IV}$O$_2$(bpy)$_4$]$^{3+}$ was used as catalyst, the O$_2$ yield and the turnover rate were found to be significantly lower,

[41] Shafirovich, V. Y.; Khannanov, N. K.; Shilov, A. E. *J. Inorg. Biochem.* **1981**, *15*, 113–129.

[42] Luneva, N. P.; Knerelman, E. I.; Shafirovich, V. Y.; Shilov, A. E. *J. Chem. Soc., Chem. Commun.* **1987**, 1504–1505.

[43] (a) Ramaraj, R.; Kira, A.; Kaneko, M. *Chem. Lett.* **1987**, 261–264. (b) Ramaraj, R.; Kira, A.; Kaneko, M. *Angew. Chem., Int. Ed. Engl.* **1986**, *25*, 825–827.

[44] Gobi, K. V.; Ramaraj, R.; Kaneko, M. *J. Mol. Catal.* **1993**, *81*, L7–L11.

[45] Yagi, M.; Narita, K. *J. Am. Chem. Soc.* **2004**, *126*, 8084–8085.

suggesting that the terminal water ligands of **2** are involved in the catalysis. UV–vis, XANES and EXAFS methods were utilized to characterize the state of the $Mn^{III}$–$Mn^{IV}$ dimer on Kaolin clay, and its oxidation to a $Mn^{IV}$–$Mn^{IV}$ complex. The kinetic analysis of the heterogeneous catalysis showed that the predominant $O_2$ evolution is produced by a bimolecular reaction of adsorbed **2**. Based on this result, the authors proposed that the close proximity of the adsorbed molecules on the Kaolin clay facilitates $O_2$ evolution.

Water oxidation catalysis by Ru ammine complexes in a Nafion membrane has been demonstrated using $Ce^{IV}$ as oxidant.[46] The complexes can work as active water oxidation catalysts in the membrane as well as in solution. Significantly, bimolecular decomposition of the catalysts, which has been found to deactivate them, was remarkably suppressed by incorporating them into the membrane, leading to high activities at high concentrations.

One of this ammine complexes, $[(NH_3)_3Ru^{III}(\mu\text{–}Cl)_3Ru^{II}(NH_3)_3]^{2+}$, constitutes the most active molecule–based water oxidation catalyst studied to date. From kinetic analysis based on the competitive reactions of water oxidation and bimolecular decomposition of the catalyst, the first–order rate constants for $O_2$ evolution in a Nafion membrane and in solution were determined as $6.3 \times 10^{-2}$ $s^{-1}$ and $5.6 \times 10^{-2}$ $s^{-1}$, respectively.[46d] The similar value of these constants shows that incorporation of the complex into the membrane does not cause a significant loss of its intrinsic activity. On the contrary, the second–order rate constant for deactivation by molecular decomposition ($8.4$ $dm^3$ $mol^{-1}$ $s^{-1}$) in the membrane is lower than that ($1.4$ $dm^3$ $mol^{-1}$ $s^{-1}$) in solution by 17 times. In this system, the cationic complex is electrostatically attached to anionic sulfonate groups on the Nafion chain, so that there is a strong restriction for the complex to diffuse in the membrane. The bimolecular decomposition would be suppressed by such restriction of the diffusion, resulting in the lower $k_{deact}$ value of the heterogeneous system.

---

[46] (a) Yagi, M.; Kasamastu, M.; Kaneko, M. *J. Mol. Catal. A, Chem.* **2000**, *151*, 29–35. (b) Yagi, M.; Sukegawa, N.; Kaneko, M. *J. Phys. Chem. B* **2000**, *104*, 4111–4114. (c) Nagoshi, K.; Yagi, M.; Kaneko, M. *Bull. Chem. Soc. Jpn.* **2000**, *73*, 2193. (d) Yagi, M.; Osawa, Y.; Sukegawa, N.; Kaneko, M. *Langmuir* **1999**, *15*, 7406–7408. (e) Yagi, M.; Sukegawa, N.; Kasamastu, M.; Kaneko, M. *J. Phys. Chem. B* **1999**, *103*, 2151–2154. (f) Yagi, M.; Nagoshi, K.; Kaneko, M. *J. Phys. Chem. B* **1997**, *101*, 5143–5146. (g) Yagi, M.; Tokita, S.; Nagoshi, K.; Ogino, I.; Kaneko, M. *J. Chem. Soc., Faraday Trans.* **1996**, *92*, 2457–2461.

Wada *et al.*[47] have reported an effective oxidation of water that is catalyzed by the indium-tin-oxide (ITO) electrode modified with the dinuclear complex $[Ru^{II}_2(OH)_2(3,6-$ *t*Bu$_2$qui)$_2$(btpyan)](SbF$_6$)$_2$ (3,6-*t*Bu$_2$qui = 3,6-di(*tert*-butyl)-1,2-benzoquinone, btpyan = 1,8-bis{(2,2':6',2")-terpyridyl}anthracene, see **Figure 9**) in water. The authors propose that both, the ruthenium centers and the quinone ligands, contribute to the four-electron oxidation of two water molecules.
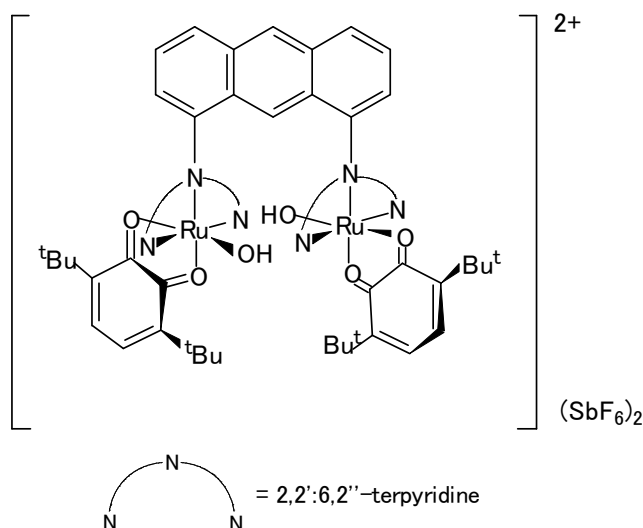


**Figure 9.** Structure of a bis-hydroxo Ru dimer able to catalyze water oxidation.[47]

## 2.3.2- Homogeneous water oxidation by manganese complexes.

Naruta *et al.*[48] detected oxygen evolution by a manganese dimer containing two covalently linked Mn$^{III}$-porphyrin units (**Figure 10a**), which was reported to be capable of catalyzing the electrochemical oxidation of water at potentials above 1.2 V *vs*. Ag/Ag$^+$. Since the number of electrons involved in the O$_2$ evolution was determined to be approximately 4 and because the Mn porphyrin dimer showed no catalase activity, the authors proposed a four-electron oxidation of water that may involve (LMn$^V$=O)$_2$ and LMn$^{IV}$-O-O-Mn$^{IV}$L as intermediates. Several Mn porphyrin dimers were later shown to catalyze olefin

---

[47] (a) Wada, T.; Tsuge, K.; Tanaka, K. *Inorg. Chem.* **2001**, *40*, 329. (b) Wada, T.; Tsuge, K.; Tanaka, K. *Angew. Chem., Int. Ed. Engl.* **2000**, *39*, 1479-1482.

epoxidation,[49] thus supporting the assignment of $Mn^V=O$ intermediates.

The electrochemically generated $(LMn^V=O)_2$ species has not yet been characterized. However, this species has been generated chemically by oxidation of the dimanganese porphyrin dimer using $m$-CPBA as oxidant, and has been subsequently characterized by UV–vis and resonance Raman spectroscopy.[50] In contrast to the low stability of monomeric $Mn^V=O$ porphyrin species under similar conditions,[51] the proposed $(LMn^V=O)_2$ was stable for hours, before decaying to a $Mn^{III,III}$ dimer following a first-order pathway ($t_{1/2}$ = 3.1 h). The authors noted that the rigid framework of the ligand, composed of two triphenylporphyrins linked by a 1,2–phenylene bridge, and the resulting long metal–metal separation (> 6 Å)[52] prevent inward bending and therefore prevent bridging of the two Mn ions via $\mu$-oxo or $\mu$-hydroxo groups; this fact, the authors argued, accounts for the extra stability of the $Mn^{V,V}$ dimer. Upon addition of an acid ($CF_3SO_3H$), a solution of the $Mn^{V,V}$ dimer gives off $O_2$ with statistical incorporation of $^{18}O$-label from the solution. The O–O bond formation could either involve the intramolecular coupling of two $Mn^V=O$ moieties, or direct attack of a water molecule on a $Mn^V=O$ group.

[48] Naruta, Y.; Sasayama, M.; Sasaki, T. *Angew. Chem., Int. Ed. Engl.* **1994**, *33*, 1839.

[49] Ichihara, K.; Naruta, Y. *Chem. Lett.* **1998**, *27*, 185–186.

[50] Shimazaki, Y.; Nagano, T.; Takesue, H.; Ye, B. H.; Tani, F.; Naruta, Y. *Angew. Chem., Int. Ed. Engl.* **2004**, *43*, 98–100.

[51] (a) Jin, N.; Bourassa, J. L.; Tizio, S. C.; Groves, J. T. *Angew. Chem., Int. Ed. Engl.* **2000**, *39*, 3849. (b) Jin, N.; Groves, J. T. *J. Am. Chem. Soc.* **1999**, *121*, 2923–2924. (c) Groves, J. T.; Lee, J. B.; Marla, S. S. *J. Am. Chem. Soc.* **1997**, *119*, 6269–6273.

[52] Shimazaki, Y.; Takesue, H.; Chishiro, T.; Tani, F.; Naruta, Y. *Chem. Lett.* **2001**, *30*, 538–539.
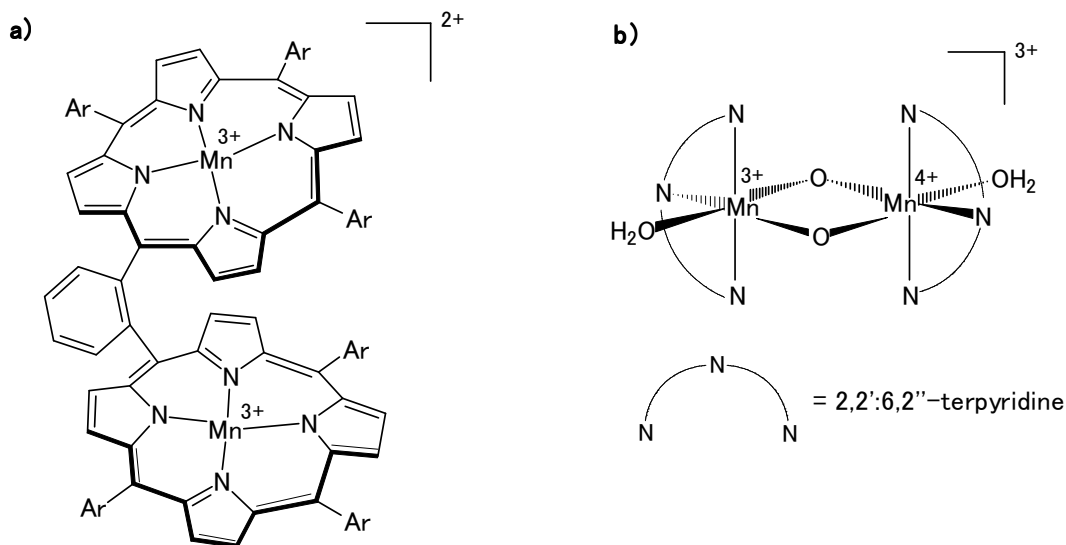
**Figure 10.** Structure of two complexes that are capable of carrying out water oxidation: a) Mn porphyrin dimer[48] and b) di–μ–oxo manganese dimer[53].

More recently, Limburg and coworkers[53] synthesized and structurally characterized a manganese dimer with terpyridine ligands, $[(trpy)(H_2O)Mn(\mu-O)_2Mn(trpy)(H_2O)]^{3+}$ (**Figure 10b**), which catalyzes oxygen evolution in the presence of an oxygen–atom transfer reagent like $KHSO_5$ (oxone) or $NaOCl$ (sodium hypochlorite). This complex is of particular interest since the unit $Mn(\mu-O)_2Mn$ is known to be part of the OEC.

Experiments of gas phase stable isotope ratio mass spectrometry were performed in $^{18}O$–enriched water to precisely determine the $^{18}O$–isotope content of the evolved $O_2$, using oxone as the oxidant, which does not exchange with water. Incorporation of $^{18}O$–label from the $^{18}O$–enriched water into the evolved $O_2$ was observed, and the extent of label incorporation was found to be dependent on the oxone concentration, supporting a pathway model that involves the attack of a $Mn^V=O$ intermediate by either oxone or water (**Figure 11**).

---

[53] (a) Limburg, J.; Vrettos, J. S.; Chen, H.; de Paula, J. C.; Crabtree, R. H.; Brudvig, G. W. *J. Am. Chem. Soc.* **2001**, *123*, 423–430. (b) Limburg. J.; Vrettos, J. S.; Liable–Sands, L. M.; Rheingold, A. L.; Crabtree, R. H.; Brudvig, G. W. *Science* **1999**, *283*, 1524.
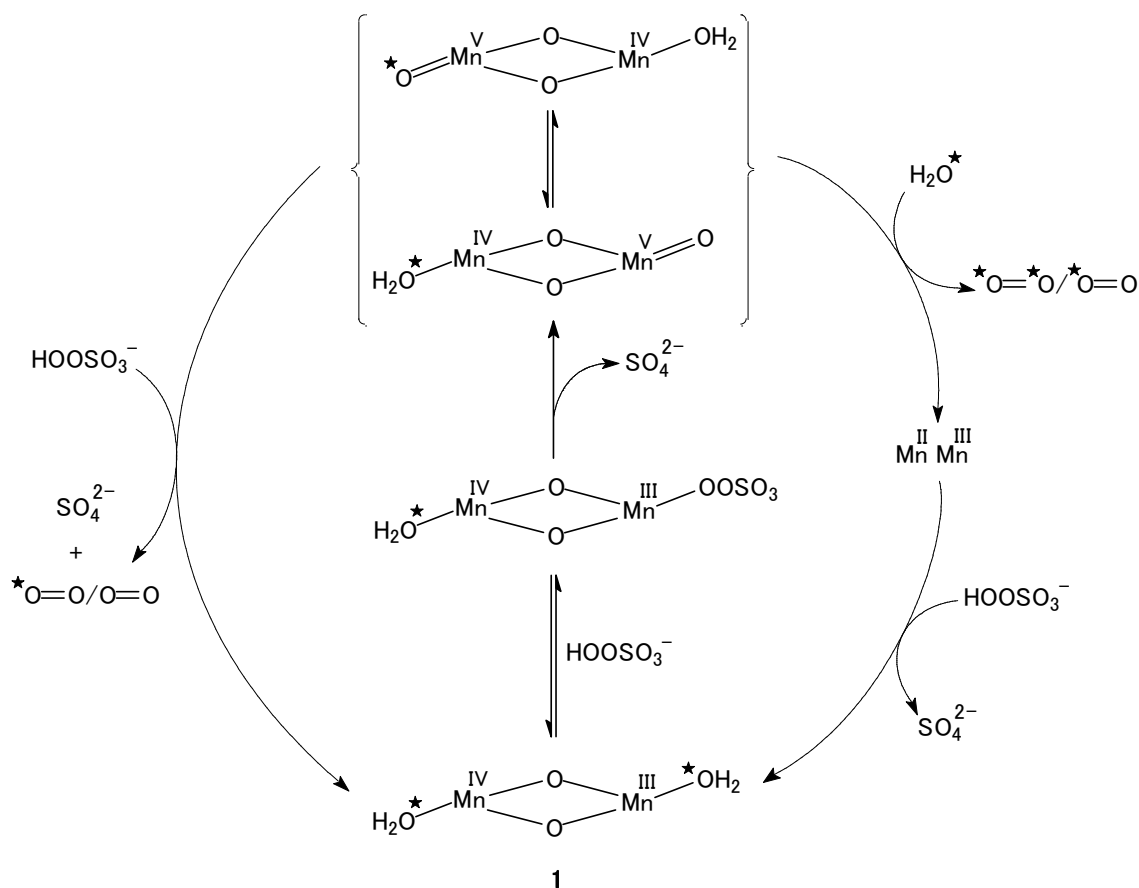
**Figure 11.** Proposed mechanism for the catalytic $O_2$ evolution with [(trpy)(H$_2$O)Mn$^{III}$(μ–O)$_2$Mn$^{IV}$(trpy)(H$_2$O)]$^{3+}$.[53a] The " * " signs mark the oxygen atoms that are originated from water, which are slightly enriched with $^{18}$O in the labeling studies.

## 2.3.3– Homogeneous water oxidation by ruthenium complexes.

In 1982, Meyer's group reported the catalytic oxidation of water and chloride with a binuclear Ru complex known as the *blue dimer*, [(bpy)$_2$(H$_2$O)RuORu(H$_2$O)(bpy)$_2$]$^{4+}$.[31] Oxidative degradation and water–anion ligand exchange of the catalyst, however, limit its activity to 10–25 turnovers. Since then, this complex and related compounds[54] have been extensively studied in order to elucidate their mechanism of water oxidation and increase

[54] (a) Petach, H. H.; Elliott, C. M. *J. Electrochem. Soc.* **1992**, *139*, 2217. (b) Comte, P.; Nazeeruddin, M. K.; Rotzinger, F. P.; Frank, A. J.; Gratzel, M. *J. Mol. Catal.* **1989**, *52*, 63–84. (c) Nazeeruddin, M. K.; Rotzinger, F. P.; Comte, P.; Gratzel, M. *J. Chem. Soc., Chem. Commun.* **1988**, 872. (d) Rotzinger, F. P.; Munavalli, S.; Comte, P.; Hurst, J. K.; Gratzel, M.; Pern, F.–J.; Frank, A. J. *J. Am. Chem. Soc.* **1987**, *109*, 6619.

their efficiency and stability.

Ramaraj *et al.* reported the catalytic activity of a number of mono-, di- and trinuclear ammine complexes.[55] Water oxidation catalysis by these complexes was investigated in homogeneous aqueous solution to evaluate the influence of structure on their catalytic activity and mechanism.[46]

The catalytic activities of various Ru complexes are summarized in **Table 1**. Comparison between multinuclear and mononuclear complexes shows that the former are more active catalysts than the latter. This is probably because the multinuclear structures are capable of forming oxidized intermediates with four delocalized oxidizing equivalents compared with only two oxidizing equivalents in the mononuclear complexes.

As for the mononuclear complexes, the sequence of the catalytic activity was *cis*-$[Ru(NH_3)_4Cl_2]^+$ >> $[Ru(NH_3)_5Cl]^{2+}$ >> $[Ru(NH_3)_6]^{3+}$, showing that the activity of the complex increases remarkably on substitution of ammine ligands by chloro ligands. Although the high catalytic activity of *cis*-$[Ru(NH_3)_4Cl_2]^+$ might be explained by its four-electron oxidation ability,[46a] the comparison between $[Ru(NH_3)_6]^{3+}$ and $[Ru(NH_3)_5Cl]^{2+}$, both of which work as only two-electron oxidation catalysts, requires further interpretation and remains a problem for future resolution.

---

[55] (a) Ramaraj, R.; Kaneko, M.; Kira, A. *Bull. Chem. Soc. Jpn.* **1991**, *64*, 1028. (b) Ramaraj, R.; Kira, A.; Kaneko, M. *J. Chem. Soc., Chem. Commun.* **1987**, 227–228. (c) Ramaraj, R.; Kira, A.; Kaneko, M. *Angew. Chem., Int. Ed. Engl.* **1986**, *25*, 1009. (d) Ramaraj, R.; Kira, A.; Kaneko, M. *J. Chem. Soc., Chem. Commun.* **1986**, 1707–1709.

**Table 1.** Comparison of the catalytic activity ($k_{O2}$) of various ruthenium complexes in water oxidation.

| SYSTEM | $k_{O2}/10^{-3}$ $s^{-1}$ [a] | |
| --- | --- | --- |
| | Homogeneous system[b] | Heterogeneous system[c] |
| $[(NH_3)_5Ru^{III}(\mu-O)Ru^{IV}(NH_3)_4(\mu-O)Ru^{III}(NH_3)_5]^{6+}$ [46g] | 51 | 45 |
| $[(bpy)_2(H_2O)Ru^{III}(\mu-O)Ru^{III}(H_2O)(bpy)_2]^{4+}$ [56] | 4.2 | 2.4 |
| $[(NH_3)_5Ru^{III}(\mu-O)Ru^{III}(NH_3)_5]^{4+}$ [46c] | 13 | 13 |
| $[(NH_3)_3Ru^{III}(\mu-Cl)_3Ru^{II}(NH_3)_3]^{2+}$ [46d] | 56 | 63 |
| $[Ru^{III}(NH_3)_6]^{3+}$ [46e] | 0.014[d] | 0.035[e] |
| $[Ru^{III}(NH_3)_5Cl]^{2+}$ [46f] | 0.31[d] | 2.7[e] |
| cis-$[Ru^{III}(NH_3)_4Cl_2]^{+}$ [46b] | 2 | 14 |
| $[Ru^{III}(en)_3]^{3+}$ [46a] | 0.17[d] | 0.085[e] |
| $IrO_2$[56] | | 1.4[f] |
| $RuO_2$[56] | | 0.75[f] |
| Pt−black[56] | | 0.25[f] |

[a]Turnover rate calculated from kinetic analysis based on first−order $O_2$ evolution and second−order deactivation. [b]Aqueous solution. [c]Nafion membrane. [d]Maximum turnover rate at a low concentration in an aqueous solution. [e]Intrinsic catalytic activity obtained by an activity analysis based on the molecular distribution. [f]Suspension system.

### 2.3.3.1− Homogeneous water oxidation catalyzed by the *blue dimer*.

Since T. J. Meyer *et al.* reported the catalytic activity of the *blue dimer*, there have been many studies on the mechanism of this catalysis with $Ce^{IV}$ or $Co^{III}$ as oxidants.[31,56,57,58] So

[56] Nagoshi, K.; Yamashita, S.; Yagi, M.; Kaneko, M. *J. Mol. Catal. A, Chem.* **1999**, *144*, 71−76.

[57] (a) Meyer, T. J.; Huynh, M. H. V. *Inorg. Chem.* **2003**, *42*, 8140−8160. (b) Yamada, H.; Koike, T.; Hurst, J. K. *J. Am. Chem. Soc.* **2001**, *123*, 12775−12780. (c) Binstead, R. A.; Chronister, C. W.; Ni, J. F.; Hartshorn, C. M.; Meyer, T. J. *J. Am. Chem. Soc.* **2000**, *122*, 8464. (d) Chronister, C. W.; Binstead, R. A.; Ni, J. F.; Meyer, T. J.

far, only the species with oxidation state $Ru^{III}(\mu-O)Ru^{III}$ and $Ru^{III}(\mu-O)Ru^{IV}$ have been characterized by X-ray crystallography,[57m,57e] while the higher oxidation state species $Ru^{IV}(\mu-O)Ru^{IV}$, $Ru^{IV}(\mu-O)Ru^{V}$ and $Ru^{V}(\mu-O)Ru^{V}$ have been characterized by UV-vis, resonance Raman and EPR spectroscopy.[57c,57e,57f,57g] It is generally believed that a species with a $O=Ru^{V}(\mu-O)Ru^{V}=O$ core is generated before the key O-O bond formation; the ruthenium terminal oxo bond ($Ru^{V}=O$) was characterized in solution by a resonance Raman band shift from 818 to 780 cm$^{-1}$ upon $^{18}O$-isotope labeling.[57b] This intermediate was also isolated as a $ClO_4^-$ salt under cold and strong acidic conditions, although handling of this compound is difficult owing to its instability.[57c]

Geselowitz and Meyer prepared $^{18}O$-labeled $Ru^{III}ORu^{IV}$ and oxidized it in $^{16}OH_2$ and 0.1 M $CF_3SO_3H$ with $Ce^{IV}$.[57i] The product distribution $^{36}O_2:^{34}O_2:^{32}O_2$ was found to be 13:64:23. These results are qualitatively consistent with a bimolecular mechanism. Based on these data and stopped-flow kinetic measurements, Meyer and coworkers proposed a bimolecular reaction in which the key O-O bond forming step involves the coupling of two $O=Ru^{V}(\mu-O)Ru^{V}=O$ species, giving $O_2$, $Ru^{V}(\mu-O)Ru^{IV}$ and $Ru^{III}(\mu-O)Ru^{IV}$ as a result (**Scheme 3a**).[57a,57c] They also mentioned the possibility that multiple pathways for water oxidation may contribute to the overall mechanism; the bimolecular mechanism, an intramolecular mechanism (**Scheme 3b**) and direct water attack on an oxo group are all reasonable pathways that could operate.

*Inorg. Chem.* **1997**, *36*, 3814-3815. (e) Schoonover, J. R.; Ni, J. F.; Roecker, L.; Whiter, P. S.; Meyer, T. J. *Inorg. Chem.* **1996**, *35*, 5885-5892. (f) Lei, Y. B.; Hurst, J. K. *Inorg. Chim. Acta* **1994**, *226*, 179-185. (g) Lei, Y. B.; Hurst, J. K. *Inorg. Chem.* **1994**, *33*, 4460-4467. (h) Hurst, J. K.; Zhou, J. Z.; Lei, Y. B. *Inorg. Chem.* **1992**, *31*, 1010-1017. (i) Geselowitz, D.; Meyer, T. J. *Inorg. Chem.* **1990**, *29*, 3894-3896. (j) Raven, S. J.; Meyer, T. J. *Inorg. Chem.* **1988**, *27*, 4478-4483. (k) Nazeeruddin, M. K.; Rotzinger, F. P.; Comte, P.; Gratzel, M. *J. Chem. Soc., Chem. Commun.* **1988**, 872-874.

**a) Bimolecular pathway**

**b) Intramolecular pathway**
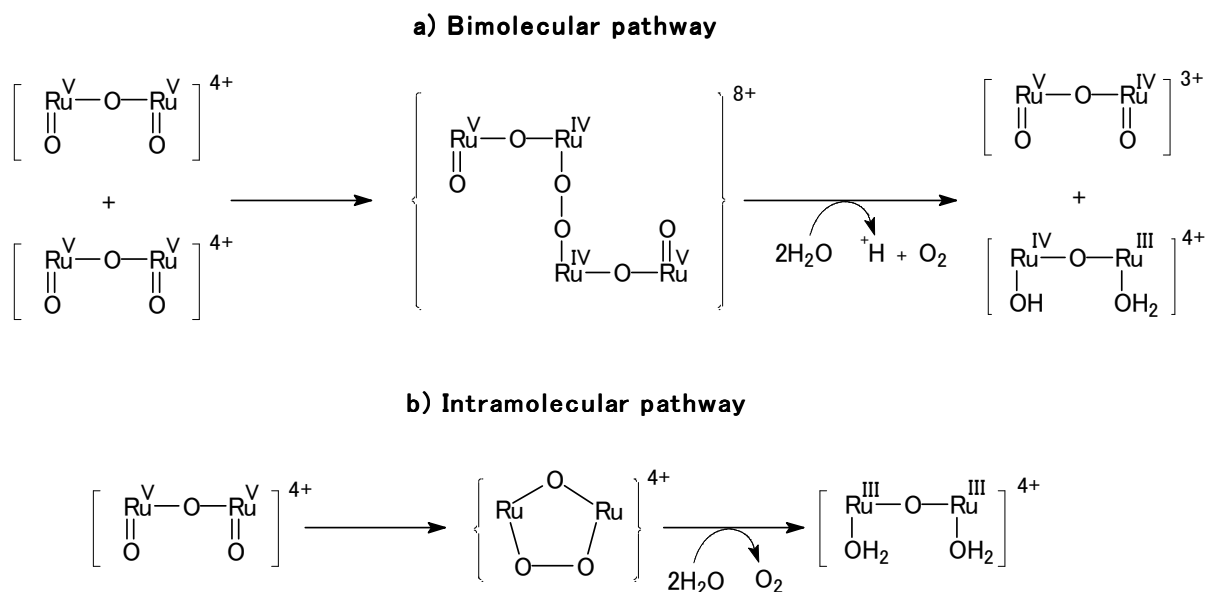
**Scheme 3.** Mechanism for O–O bond formation proposed by T. J. Meyer and coworkers. Scheme adapted from reference 57c.

Similar $^{18}$O–labeling/MS experiments were carried out by Hurst and coworkers using Co$^{III}$ and Ce$^{IV}$ as oxidants in $CF_3SO_3H$ aqueous solutions.[57h,58] However, they obtained only trace amounts of $^{36}O_2$, in contrast with the aforementioned results by Geselowitz and Meyer, who obtained significant relative yields of $^{36}O_2$.

Taking into account these results and the measured temperature and deuterium solvent isotope dependencies of the $O_2$ evolution rate, Hurst *et al.* proposed recently a mechanism involving two reaction pathways, both of which involve nucleophilic addition of water to the Ru complex. Such addition can be either direct to Ru$^V$=O forming Ru–O–OH, or can involve the oxidized form of bpy as intermediate (**Scheme 4**).[58]

[58] Yamada, H.; Siems, W. F.; Koike, T.; Hurst, J. K. *J. Am. Chem. Soc.* **2004**, *126*, 9786–9795.
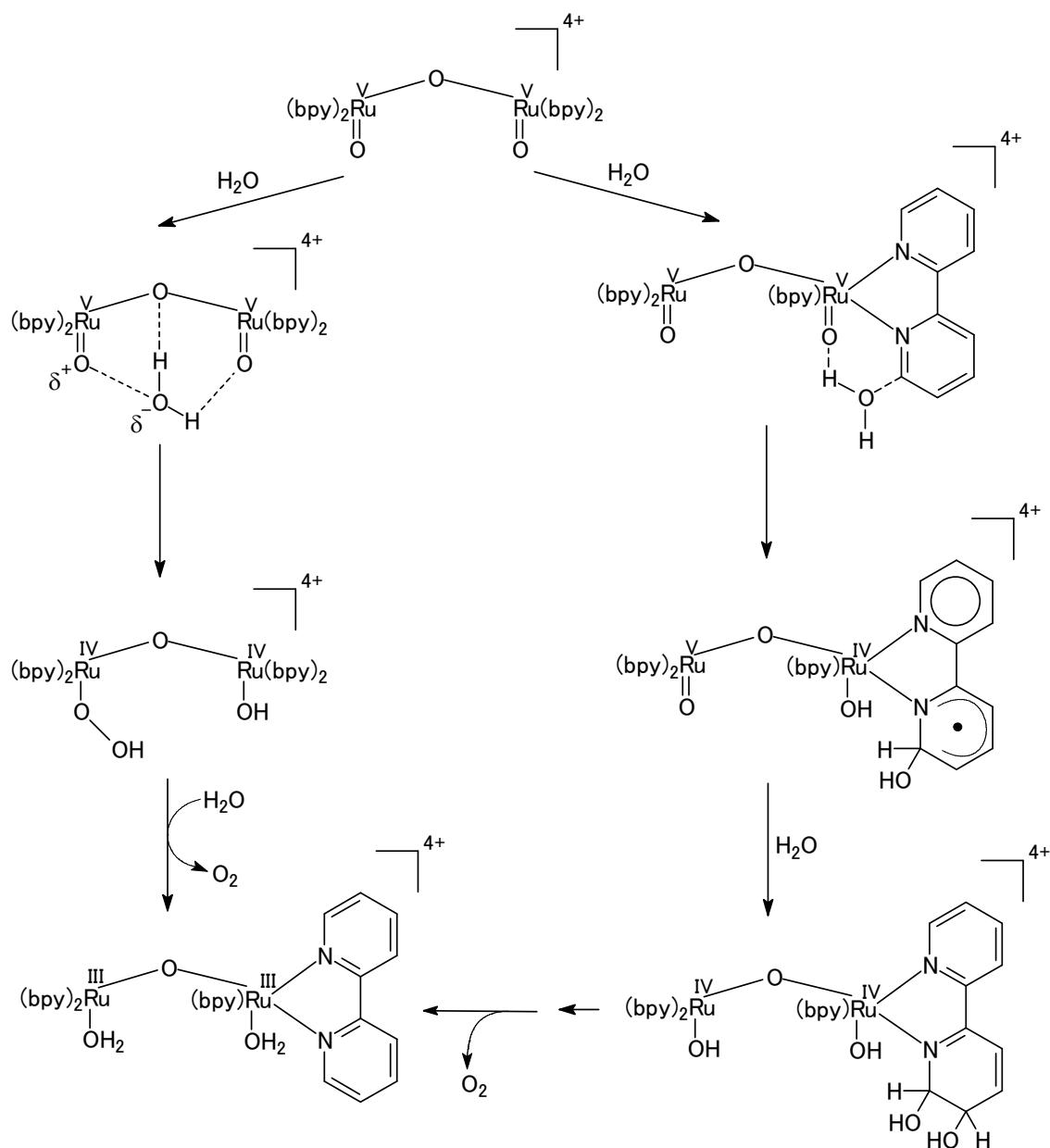
**Scheme 4.** Mechanism for O–O bond formation proposed by Hurst and coworkers. Scheme adapted from reference 58.

Unfortunately, the catalytic cycle of the *blue dimer* is further complicated by anion binding, which inhibits $O_2$ evolution and slows down the overall catalysis because the rate-limiting step becomes water replacement of the coordinated anion.[57c]

# OBJECTIVES

The 3,5-bis(2-pyridyl)pirazole ligand (Hbpp) is considerably versatile from both acid-base and synthetic viewpoints. It contains two pyridyl groups which can be protonated at acid pH when they are not coordinated to a metal and a pirazole ring which can be deprotonated at basic pH, allowing the formation of dimeric structures where the two metal centers are in close proximity.
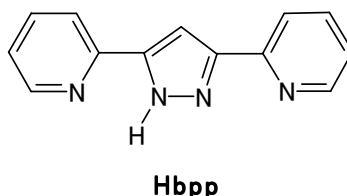


**Hbpp**

This versatility prompted us to synthesize new mono- and dinuclear ruthenium complexes containing this ligand. We were first interested in the synthesis of complexes containing Hbpp and dmso. The ambidentate nature of dmso can induce linkage isomerization reactions when going from Ru$^{II}$ to Ru$^{III}$ which can be studied by means of cyclic voltammetry. Moreover, ruthenium dmso complexes are known to act as antitumoral and antimetastatic agents and are good starting materials for the synthesis of other complexes where the dmso ligands are replaced by others, e.g., polypyridylic ligands.

Ruthenium aqua complexes have been extensively studied as catalysts in many organic and inorganic processes. They present a rich redox chemistry derived from the acid-base properties of the aqua ligand. As Hbpp itself offers different protonation sites, we envisaged that the redox chemistry of Ru-Hbpp-aqua complexes would be particularly rich, making them especially interesting in catalysis and as pH-induced switches. Therefore, the next target of our project was the synthesis and characterization of this kind of complexes, using the previous Ru-dmso complexes as starting materials and trpy as an ancillary ligand.

In spite of intensive investigation by many research groups, so far few complexes of manganese and ruthenium have been found to act as water oxidation catalysts. Since the oxidation of water to molecular oxygen requires the loss of 4e$^-$ and 4H$^+$ with the concomitant formation of an oxygen-oxygen bond, one potential catalyst for this process would be a ruthenium dimer with two Ru-aqua units close to each other. This strategy

was shown to be successful by Meyer and coworkers in 1982 with the synthesis of the *blue dimer*.

We decided to prepare a new ruthenium aqua dimer using the deprotonated bpp⁻ as a bidentate ligand, so that two Ru-aqua units would be held in close proximity. We anticipated that the bpp⁻ chelating backbone would make this complex more stable than the *blue dimer*. On one hand, the absence of an oxo bridge in our structure would avoid decomposition by reductive cleavage. On the other hand, the negative charge of the bridging bpp⁻ would lower the overall positive charge of the active catalyst, thus disfavoring deactivation provoked by replacement of the water ligands with anions present in the media.

The objectives of this thesis can be then summarized as:

- ▸ Synthesis of new mononuclear complexes of ruthenium containing the Hbpp and dmso ligands. Structural, spectroscopic and electrochemical characterization.

- ▸ Synthesis of new mononuclear Ru complexes with trpy and Hbpp, using the previous Ru-dmso complexes as starting materials. Structural, spectroscopic and electrochemical characterization.

- ▸ Synthesis of new Ru dimers with trpy and the anionic bpp⁻ ligands. Structural, spectroscopic and electrochemical characterization. Study of their applications as catalysts in redox reactions, particularly in water oxidation to molecular oxygen.

# RESULTS AND DISCUSSION

## New mono- and dinuclear ruthenium complexes containing the 3,5-bis(2-pyridyl)pyrazole ligand. Synthesis, characterization and applications.

Mononuclear ruthenium polypyridyl complexes are known to perform a variety of inorganic and organic transformations. In particular, $Ru^{IV}=O$ complexes are used extensively as catalysts for the oxidation of organic substrates. It has been postulated that this catalytic behavior could be enhanced by coupling two adjacent metals, thus allowing for strong communication between them and perhaps a cooperative catalytic or redox behavior.

Special attention has been paid to Ru=O polypyridyl dimers as components of artificial photosynthetic systems capable of converting solar energy into fuels. The characteristics of these dimers are particularly well suited for carrying the water oxidation to molecular dioxygen that takes place in natural photosynthesis, by accepting $4e^-$ and $4H^+$ from water and forming an O-O bond. Meyer *et al.* have reported a dinuclear oxo-bridged Ru catalyst able to perform this catalysis, the so-called *blue dimer*. However, instability renders the complex barely effective as catalyst.
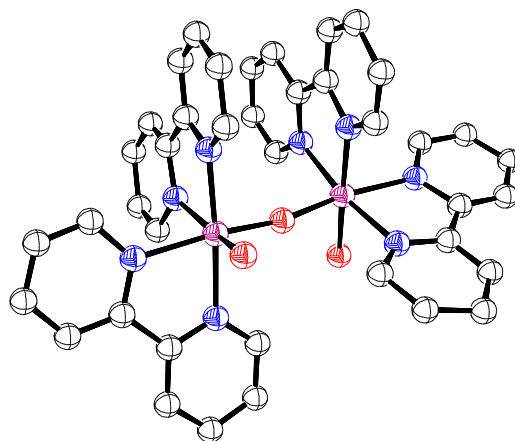


**Figure 1.** ORTEP view for the *blue dimer,* $[(bpy)_2(OH_2)Ru^{III}ORu^{III}(OH_2)(bpy)_2]^{4+}$.

With all this in mind, we decided to develop the chemistry of Ru complexes containing the 3,5-bis(2-pyridyl)pyrazole ligand (Hbpp). This ligand offers multiple protonation and coordination sites and can, therefore, form mononuclear as well as dinuclear complexes

where the two metal centers are strategically situated close to each other.



**Hbpp**
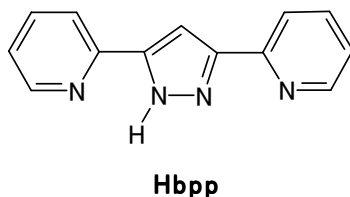
We anticipated that a Ru–OH$_2$ dimer containing this ligand would be promising for water oxidation, since it would contain two linked metal sites and two bonded water molecules held in close proximity by the bpp$^-$ chelating backbone, rendering the structure more stable than in the aforementioned *blue dimer*.

## Synthesis and characterization of new ruthenium complexes with formula [Ru$^{II}$Cl$_2$(Hbpp)(dmso)$_2$] (PAPER A).[1]

We were first interested in the synthesis of isomeric complexes having the formula [Ru$^{II}$Cl$_2$(Hbpp)(dmso)$_2$]. It seemed especially interesting to study the electrochemical properties of these complexes containing dmso, a bidentate ligand able to promote linkage isomerization reactions, and the Hbpp ligand, which leads to a pH–dependent electrochemical behavior of the corresponding complexes. These complexes could also serve as starting materials for the synthesis of other mono– and dinuclear species where the dmso ligands could be substituted by polipyridylic ligands such as bpy or trpy.

The synthesis of these compounds was performed by reacting equimolar amounts of RuCl$_2$(dmso)$_4$ and the neutral Hbpp ligand. This reaction can potentially form six different stereoisomers, including two pairs of enantiomers, which are depicted in **Figure 2**.

---

[1] Sens, C.; Rodríguez, M.; Romero, I.; Llobet, A.; Parella, T.; Sullivan, B. P.; Benet–Buchholz, J. *Inorg. Chem.* **2003**, *42*, 2040–2048.
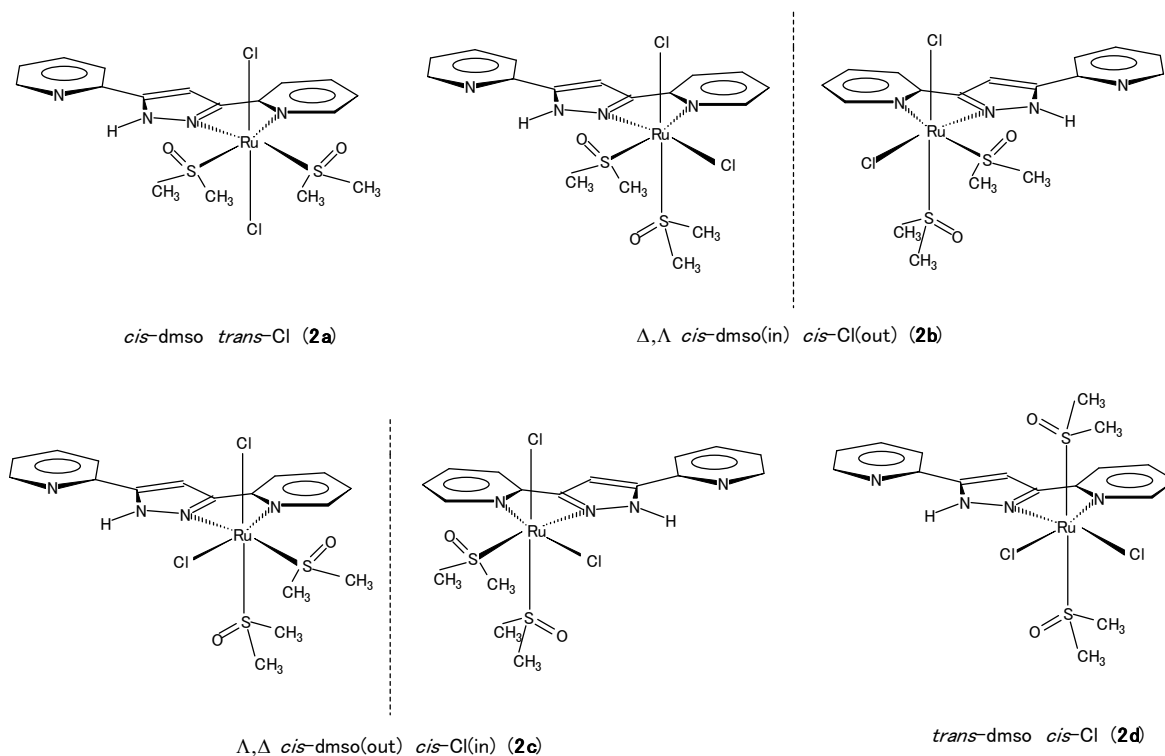
*cis*-dmso *trans*-Cl (**2a**)                    Δ,Λ *cis*-dmso(in) *cis*-Cl(out) (**2b**)

Λ,Δ *cis*-dmso(out) *cis*-Cl(in) (**2c**)

*trans*-dmso *cis*-Cl (**2d**)

**Figure 2.** Possible stereoisomers for [RuCl$_2$(Hbpp)(dmso)$_2$] (the notation *in* and *out* refers to the orientation of the equatorial Cl and dmso ligands, toward or away, respectively, from the center of Hbpp).

However, only three complexes (**2a** and the pair of enantiomers **2b**) are obtained from the reaction, which are the kinetically and thermodynamically favored isomers, respectively. This fact has been rationalized in terms of structural and electronic factors. Particularly relevant is the hydrogen bond between the inner dmso and the pyrazolylic proton (as confirmed by X-ray diffraction studies; see **Figure 3**) which explains the apparent chemical stability of **2a** and **2b** when they are compared to **2c** and **2d**.

On the other hand, the increased stability of **2b** with regard to **2a** is explained by the presence of the favorable *trans*-Cl-dmso array, as illustrated in numerous examples of the literature.
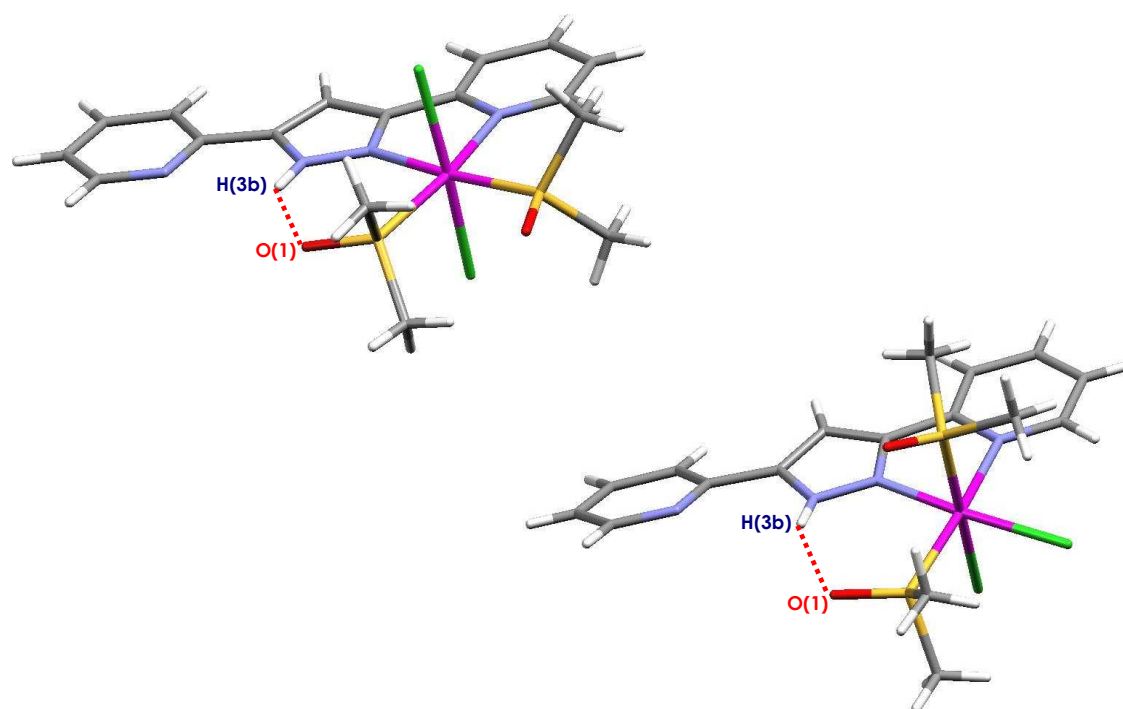
**Figure 3.** X-ray structures for **2a** (top) and **2b** (bottom) showing hydrogen bond interactions (H(3b)-O(1) = 1.98(5) Å in **2a** and 2.08(12) in **2b**).

In addition, the mentioned hydrogen bond allowed us to rationalize a significant part of the chemistry of these compounds, which were fully characterized by means of electrochemical, spectroscopic and X-ray diffraction techniques. We also studied the photochemical properties of these complexes in acetonitrile solution and their catalytical behavior in hydrogenation and hydrogen transfer type of reactions with acetophenone as substrate.

The most prominent features we encountered for both isomers are next detailed:

## A) X-ray diffraction.

The rotation of the free pyridyl group of the Hbpp ligand with regard to the central pyrazole ring is small (3.1° and 17.5° for **2a** and **2b**, respectively) due to the hydrogen bond between the nitrogen of the free pyridyl group and the aminic pyrazolyl hydrogen (**Figure 4**).
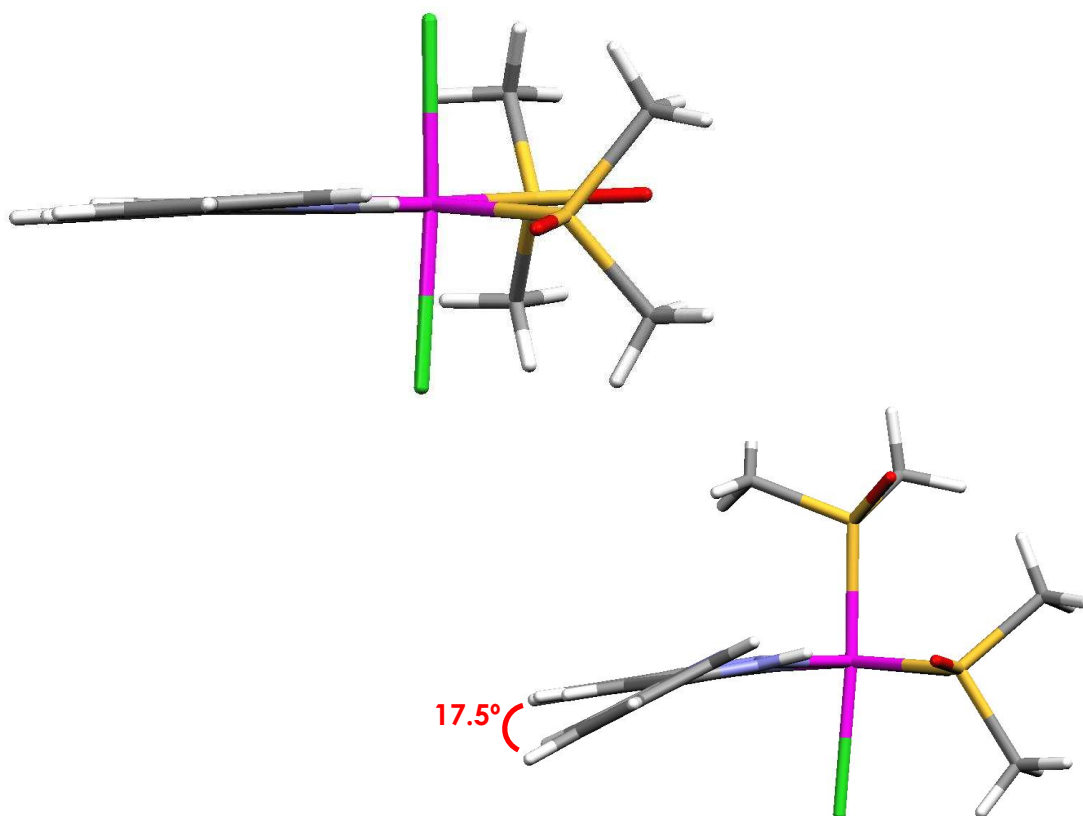
**Figure 4.** X-ray structures for **2a** (top) and **2b** (bottom) showing the rotation of the Hbpp free pyridyl group with regard to the central pyrazole ring.

## B) NMR spectroscopy.

The coordinated dmso ligands appear in the aliphatic region of the NMR spectra. For **2a**, two signals appear at 3.65 and 3.57 ppm which are assigned to the inner and the outer dmso, respectively. The equivalence of the two methyl groups of each dmso ligand indicates that a plane of symmetry that contains Hbpp and bisects the dmso molecules is present in solution. In contrast, four methyl dmso signals are observed for **2b** at 3.71, 3.69, 3.14 and 2.14 ppm due to the molecule asymmetry. The first two signals correspond to the equatorial dmso whereas the signals of the axial dmso appear at lower $\delta$ values due to the anisotropic effect of the coordinated pyridyl group of Hbpp.

## C) Photochemistry.

Exposition of an acetonitrile solution of either **2a** or **2b** to UV or sunlight for a few minutes provokes the substitution of one dmso ligand for a MeCN molecule, presumably forming

the complex *cis(out)*-[Ru$^{II}$Cl$_2$(Hbpp)(MeCN)(dmso)] (**4**) as suggested by spectrophotometric (**Figure 5**), electrochemical and NMR studies. The fact that only the non-hydrogen-bonded dmso is substituted, suggests that the presence of the hydrogen bond significantly decreases the lability of the inner dmso.
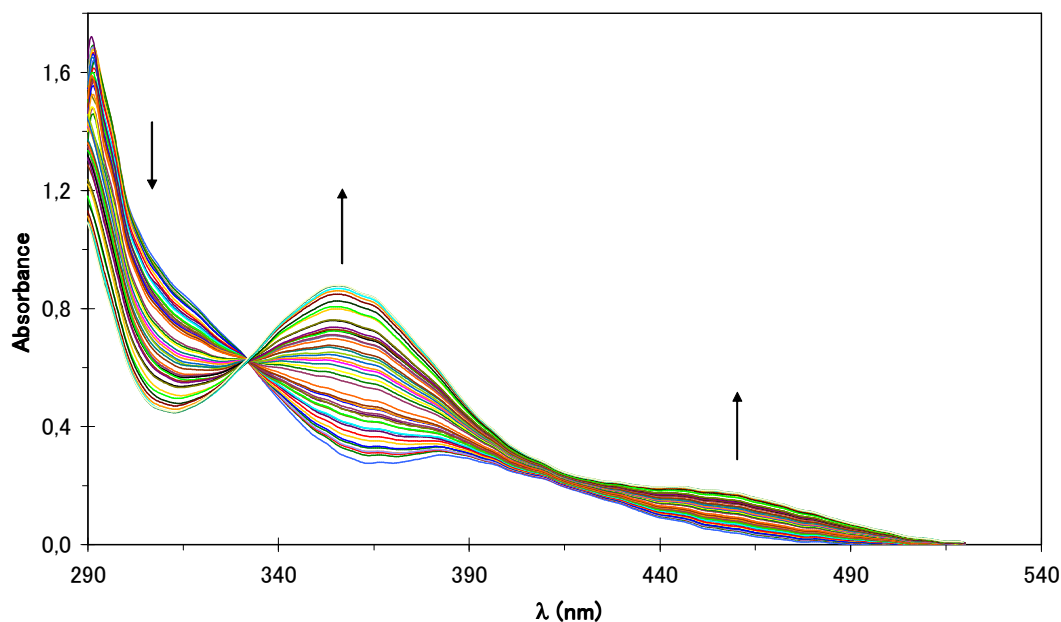


**Figure 5.** Spectral changes observed during the photochemical substitution of *trans,cis*-[RuCl$_2$(Hbpp)(dmso)$_2$] (8.356 × 10$^{-5}$ M) to *cis(out)*-[RuCl$_2$(Hbpp)(CH$_3$CN)(dmso)] in acetonitrile solution.

## D) Electrochemistry.

These compounds exhibit a complex electrochemical behavior due to the ambidentate nature of the dmso ligands and to the acid-base properties of Hbpp.

The redox properties of the two isomers, **2a** and **2b,** were studied in acetonitrile solution. As expected, a change in the pH of the media is accompanied by a change of redox potential. For **2b**, E$_{1/2}$ values of 0.425, 0.84 and 0.93 V *vs.* SSCE were obtained in basic, neutral and acidic media, respectively, for the Ru(III/II) couple. The shift of the redox potential value in basic media is due to the formation of *cis(out),cis*-[RuCl$_2$(bpp)(dmso)$_2$]$^-$ by deprotonation of the Hbpp ligand, whereas in acidic media *cis(out),cis*-[RuCl$_2$(H$_2$bpp)(dmso)$_2$]$^+$ is formed by protonation of the Hbpp free pyridyl group.

As for complex **2a**, electrochemical studies performed in acetonitrile basic media clearly demonstrate the presence of linkage isomerization reactions when $Ru^{II}$ is one-electron oxidized to $Ru^{III}$. Linkage isomerization reactions of Ru–dmso type of complexes are common, and are explained by the ambidentate nature of dmso, which can coordinate to a metal either by the sulfur or the oxygen atom. In agreement with *the Pearson's hard/soft acid/base theory*, the sulfur site is the preferred by soft atoms such as ruthenium(II), whereas the oxygen site coordination is more favorable with hard metals. As ruthenium(III) is harder than ruthenium(II), oxidation of a Ru–dmso complex from the II to the III oxidation state can induce linkage isomerization of *S*–dmso to *O*–dmso, which is the case for **2a** in basic media.

The linkage isomerization process for deprotonated **2a**, *trans,cis*–[RuCl$_2$(bpp)(dmso)$_2$]$^-$, is clearly evidenced in the cyclic voltammetry of the complex when scanning in the cathodic direction (**Figure 6**). A wave at E$_{1/2}$ = −0.200 V corresponding to *trans,cis*–[RuCl$_2$(bpp)(*O*–dmso)(*S*–dmso)]$^-$ appears, in addition to the 0.380 V due to the *trans,cis*–[RuCl$_2$(bpp)(*S*–dmso)$_2$]$^-$ analog.
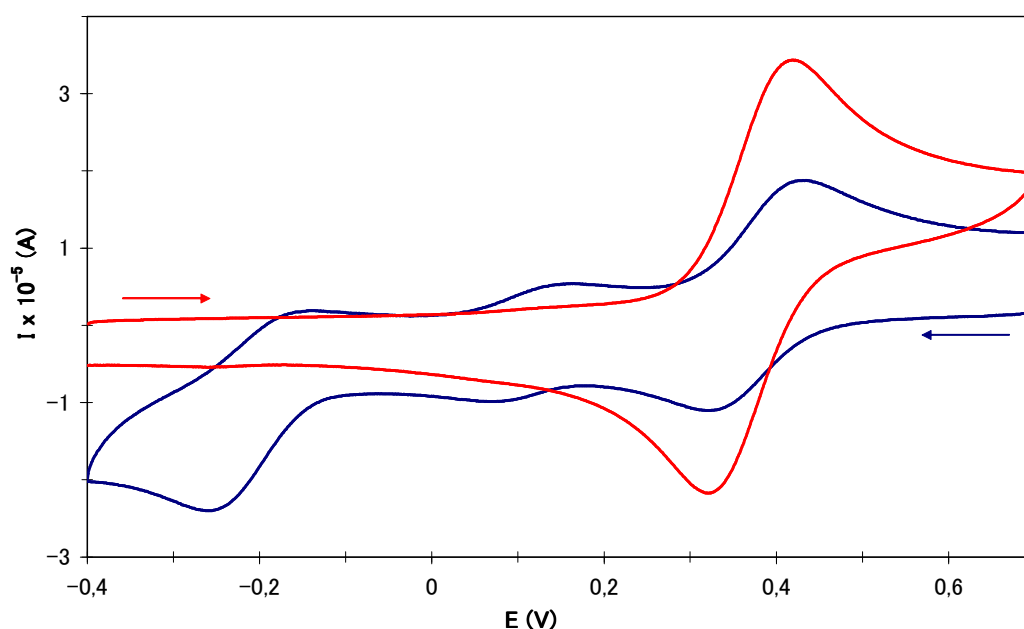


**Figure 6.** Cyclic voltammetries for **2a** 1mM in CH$_3$CN basic media starting in the anodic (red) and cathodic (blue) direction at 1 V/s.

The wave at 0.130 V is assigned to the formation of *cis(out)*-[Ru$^{II}$Cl$_2$(bpp)(MeCN)(*S*-dmso)]$^-$. The thermodynamic cycle for the process, together with the calculated thermodynamic and kinetic constant values, is depicted in **Figure 7**. These values have been estimated from the cyclic voltammograms at different scanning rates.
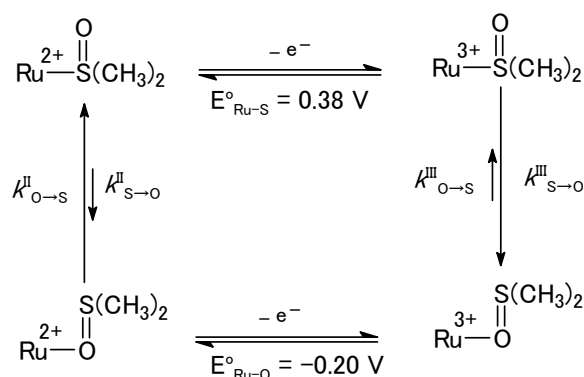
$$\begin{array}{ccc}
\text{Ru}^{2+}\!-\!\overset{\overset{\displaystyle O}{\|}}{\text{S}}(\text{CH}_3)_2 & \xrightleftharpoons[E^\circ{}_{\text{Ru-S}}=0.38\text{ V}]{-\,e^-} & \text{Ru}^{3+}\!-\!\overset{\overset{\displaystyle O}{\|}}{\text{S}}(\text{CH}_3)_2 \\[4pt]
k^{II}{}_{O\rightarrow S}\ \updownarrow\ k^{II}{}_{S\rightarrow O} & & k^{III}{}_{O\rightarrow S}\ \updownarrow\ k^{III}{}_{S\rightarrow O} \\[4pt]
\text{Ru}^{2+}\!-\!\overset{\overset{\displaystyle S(\text{CH}_3)_2}{\|}}{\text{O}} & \xrightleftharpoons[E^\circ{}_{\text{Ru-O}}=-0.20\text{ V}]{-\,e^-} & \text{Ru}^{3+}\!-\!\overset{\overset{\displaystyle S(\text{CH}_3)_2}{\|}}{\text{O}}
\end{array}$$

**Figure 7.** Thermodynamic cycle for the linkage isomerization process that takes place during the electrochemical oxidation of complex **2a** in basic media ($K^{III}{}_{O\rightarrow S}$ = 0.25 ± 0.025, $k^{III}{}_{O\rightarrow S}$ = 0.017 s$^{-1}$, $k^{III}{}_{S\rightarrow O}$ = 0.065 s$^{-1}$; $K^{II}{}_{O\rightarrow S}$ = 6.45 × 10$^9$, $k^{II}{}_{O\rightarrow S}$ = 0.132 s$^{-1}$, $k^{II}{}_{S\rightarrow O}$ = 2.1 × 10$^{-11}$ s$^{-1}$).

## E) Catalysis.

No catalytic activity was found for **2a** or **2b** in the hydrogenation of acetophenone. However, both isomers act as hydrogen transfer catalysts from 2-propanol to acetophenone, yielding 2-phenylethyl alcohol as the only product. Isomer **2a** is markedly more active in this reaction than **2b**, with 42.1% conversion with regard to acetophenone and 36.1 metal cycles at 80°C and at a catalyst:acetophenone relation of approx. 1:100. The increased activity of **2a** agrees well with the fact that it is less stable than **2b** and therefore, more prone to ligand substitution, which is the first step in the currently accepted mechanism for this reaction.

**Synthesis and characterization of new ruthenium complexes with formula *in-* and *out-* [Ru$^{II}$(Hbpp)(trpy)X]$^{n+}$ where X = Cl, H$_2$O and py (PAPER B).[2]**

As already said, ruthenium polypyridyl complexes are extensively used as catalysts for a myriad of organic and inorganic transformations, particularly when ligands having acid-base properties, such as aqua ligands, are coordinated to the metal. The redox and spectroscopic properties of this type of complexes can be fine-tuned by changing the pH, which makes them interesting for acting as tailored catalysts for specific reactions and as pH-induced switches.

Our group's extensive background in the chemistry of ruthenium polypyridyl aqua complexes, together with the rich acid-base properties of the Hbpp ligand (already evidenced in the previous Ru-dmso complexes), prompted us to synthesize three pairs of geometrical isomers with formula [Ru$^{II}$(Hbpp)(trpy)X]$^{n+}$ where X= Cl (n = 1, **2a,b**), H$_2$O (n = 2, **3a,b**) and py (n = 2, **4a,b**). The previously synthesized *cis(out),cis-*[RuCl$_2$(Hbpp)(dmso)$_2$] was used as starting material for the synthesis of the chloro compounds, by reacting it with one equivalent of trpy. Two geometrical isomers with formula [Ru$^{II}$Cl(Hbpp)(trpy)]$^+$ were obtained, which we differentiate by the prefixes *in-* and *out-* depending on whether the equatorial chloro ligand is directed toward or away, respectively, from the center of Hbpp (**Figure 8**).

Another synthetic route, using RuCl$_3$(trpy) and the protected ligand bpp-BOC as reagents, was essayed which led to higher yields of both isomers. The *out-* and *in-*aqua analogs were easily obtained by reacting the chloro isomers with equivalent amounts of AgClO$_4$ in the presence of water. As for the *in-* and *out-*pyridine complexes, they were obtained either from the chloro or the aqua analogs, by refluxing them in the presence of an excess

[2] Sens, C.; Rodríguez, M.; Romero, I.; Llobet, A.; Parella, T.; Benet-Buchholz, J. *Inorg. Chem.* **2003**, *42*, 8385-8394.
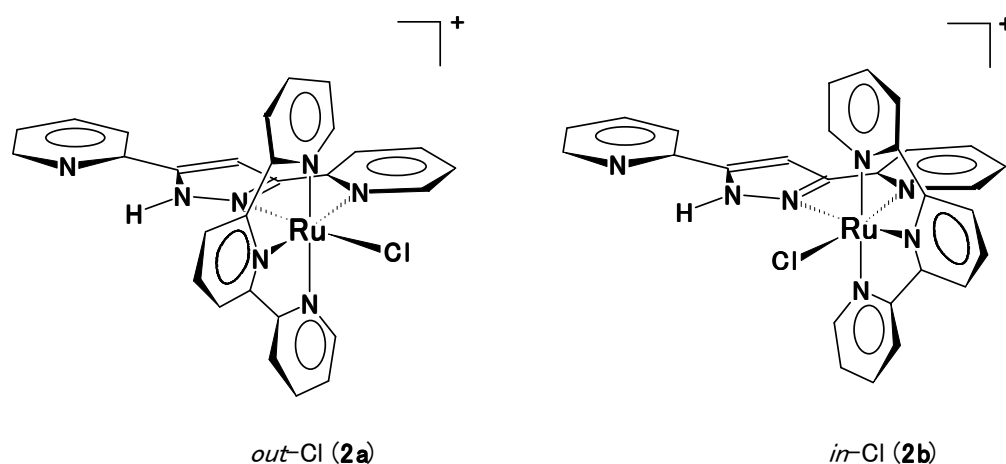
of pyridine.



out-Cl (**2a**)                              in-Cl (**2b**)

**Figure 8.** Geometrical isomers of $[Ru^{II}Cl(Hbpp)(trpy)]^+$.

## A) X-ray diffraction.

Suitable crystals for X-ray diffraction analysis were obtained for **2a**, **3a** and **4a,b**. In all cases, the Ru metal presents a pseudo-octahedral structure with the trpy ligand coordinated in a meridional manner. A differential feature of these compounds is the rotation angle of the free pyridyl group of the Hbpp ligand with regard to the central pyrazole ring (see **Table 1** and **Figure 9**).

**Table 1.** Values for the torsion angle N(4)–C(9)–C(8)–N(3) for **2a**, **3a**, **4a,b**.

| | Dihedral angle N(4)–C(9)–C(8)–N(3) (°) |
|---|---|
| out-Cl **2a** | 0 |
| out-aqua **3a** | 33.7 |
| out-py **4a** | −12.9 |
| in-py **4b** | −179.7 |

The structure shown in **Figure 9** corresponds to the hydrochloride form of **2a**, namely *out*–[Ru$^{II}$Cl(H$_2$bpp)(trpy)]Cl(PF$_6$). It is remarkable the 0° value for the dihedral angle N(4)–C(9)–C(8)–N(3) due to the hydrogen bond between the free chloride (Cl(1x)), and the hydrogen atoms bonded to N(3) and N(4) (named H(3b) and H(4b), respectively) which impedes the rotation of the free Hbpp pyridyl group.
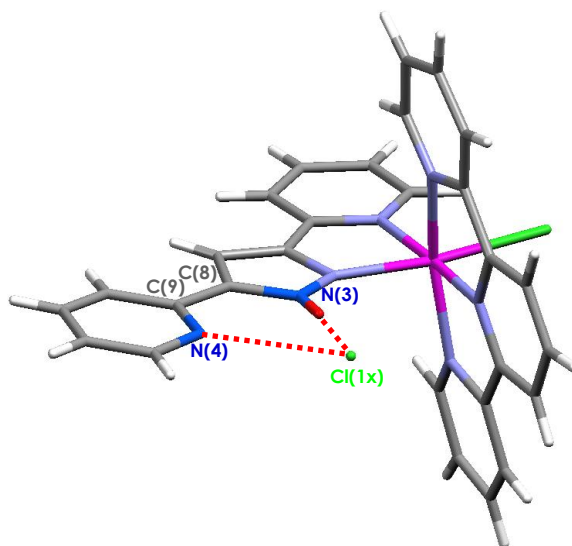


**Figure 9.** X–ray structure for **2a** showing the hydrogen bond interactions (H(3b)–Cl(1x) = 2.164 Å, Cl(1x)–N(3) = 3.035 Å, H(4b)–Cl(1x) = 2.131 Å, Cl(1x)–N(4) = 3.009 Å).

In the Ru–OH$_2$ complex **3a**, the corresponding dihedral angle is 33.7°. The molecules of this compound build a dimer with *C*2–symmetry due to the hydrogen bond interactions which take place between the pyrazolyl proton of one molecule (H(3)) and the nitrogen of the noncoordinated pyridyl ring of the neighboring molecule (N(4')) (N(3)–N(4') = 2.828 Å and N(4)–H(3') = 2.025 Å).

As for the pyridine complexes, the −179.7° rotation value for the free pyridyl group of the *in*–isomer **4b** contrasts with the analog value for *out*–**4a**, which is only −12.9°. We attribute this difference to the presence of a hydrogen bond in **4a** that takes place between a solvated water molecule (O(1w), H(1w)), the aminic hydrogen of the pyrazole (H(3n)) and the noncoordinated pyridyl group (N(4)) (**Figure 10**) (H(1w)–N(4) = 1.756 Å, N(4)–O(1w) = 2.716 Å, H(3n)–O(1w) = 1.924 Å, O(1w)–N(3) = 2.760 Å).
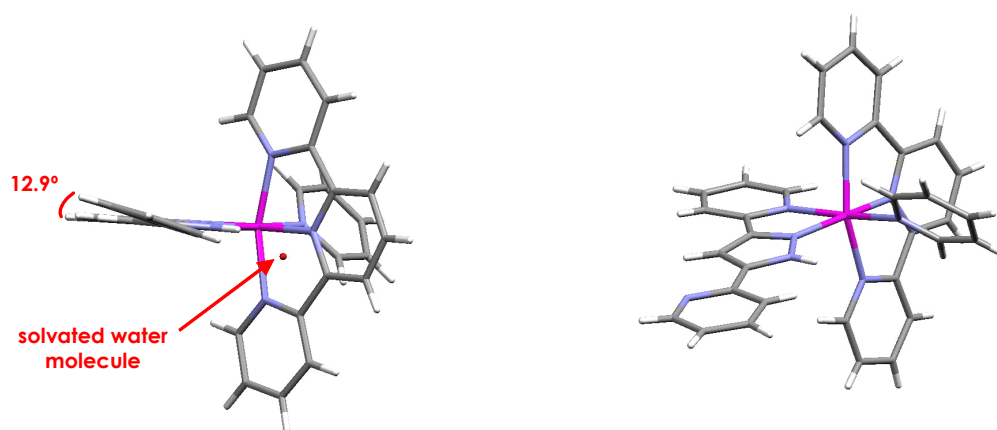
**Figure 10.** X-ray structure for **4a** (left) and **4b** (right) showing the rotation of the Hbpp free pyridyl group with regard to the central pyrazole ring.

## B) UV-vis spectroscopy.

The spectroscopic properties of the complexes depend on the pH of the solution, as expected for ruthenium complexes containing ligands with acid-base properties. Particularly interesting is the dependence of the Ru-aqua complexes on the pH of the media, since they have three sites that can be protonated or deprotonated within the pH range 0–13: the noncoordinated pyridyl group (pyr), the pyrazolyl group (pzH) and the bonded water molecule. Spectrophotometric acid-base titrations of **3a** and **3b** were carried out to precisely determine the p$K_a$ values that follow (**Table 2**):

**Table 2.** p$K_a$ values for the three successive deprotonations of Ru$^{II}$ species **3a** and **3b**.

|  | p$K_{ai}$(Ru$^{II}$) | |
|---|---|---|
|  | *out*-**3a** | *in*-**3b** |
| (i = 1) [Ru$^{II}$(**H$_2$bpp**)(trpy)(H$_2$O)]$^{3+}$ → [Ru$^{II}$(**Hbpp**)(trpy)(H$_2$O)]$^{2+}$ + H$^+$ | 2.13 | 1.96 |
| (i = 2) [Ru$^{II}$(**Hbpp**)(trpy)(H$_2$O)]$^{2+}$ → [Ru$^{II}$(**bpp**)(trpy)(H$_2$O)]$^+$ + H$^+$ | 6.88 | 7.43 |
| (i = 3) [Ru$^{II}$(bpp)(trpy)(**H$_2$O**)]$^+$ → [Ru$^{II}$(bpp)(**OH**)(trpy)] + H$^+$ | 11.09 | 12.20 |

The p$K_{a1}$ values are similar for both isomers, whereas the values of p$K_{a2}$ and p$K_{a3}$ indicate that **3b** is less acidic. We attribute this to the hydrogen bonding between the coordinated water molecule and the pyrazolyl group that can take place in the *in*–isomer.

### C) Redox properties.

The pH–dependent redox properties of the complexes are evidenced in their Pourbaix diagram. **Figure 11** shows the corresponding diagram for **3a**.
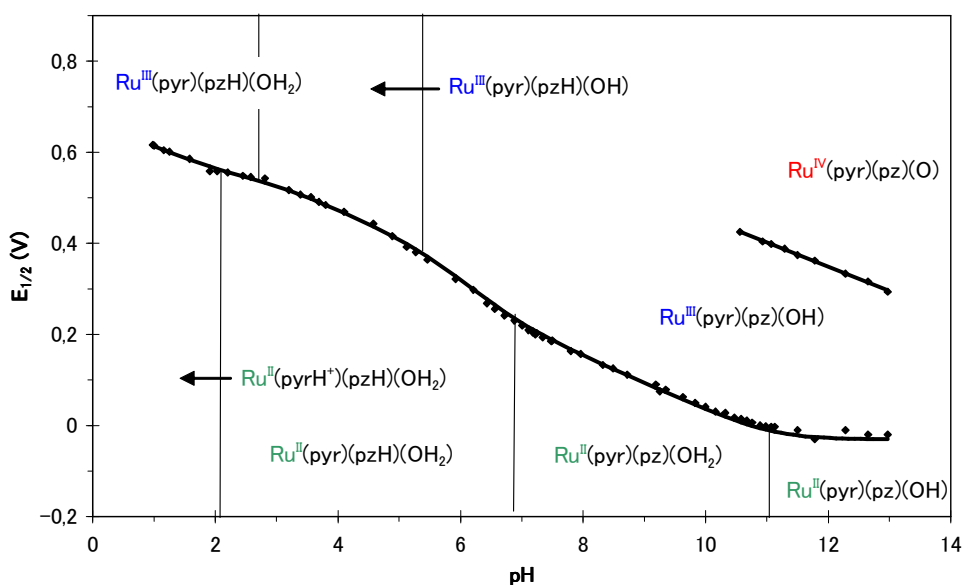


**Figure 11.** Pourbaix diagram for **3a**. The pH–potential regions of stability for the various oxidation states and their dominant proton compositions are indicated. The p$K_a$ values are shown by the vertical solid lines in the various E–pH regions.

The curves of the graphic were obtained by nonlinear least–squares analysis of the experimental data, using the mathematical expression of $E_{1/2}$(III/II) as a function of $[H^+]$ and the p$K_{ai}$ (Ru$^{II}$, i = 1, 2 and 3) values reported in **Table 2**. The values of p$K_{ai}$(Ru$^{III}$) obtained are indicated in **Table 3**.

**Table 3.** p$K_a$ values for the three successive deprotonations of $Ru^{III}$ species **3a** and **3b**.

| | p$K_{ai}$($Ru^{III}$) | |
|---|---|---|
| | *out*-**3a** | *in*-**3b** |
| **(i = 1)** $[Ru^{III}(H_2bpp)(trpy)(H_2O)]^{4+} \rightarrow [Ru^{III}(Hbpp)(trpy)(H_2O)]^{3+} + H^+$ | ~ 0 | ~ 0 |
| **(i = 2)** $[Ru^{III}(Hbpp)(trpy)(H_2O)]^{3+} \rightarrow [Ru^{III}(OH)(Hbpp)(trpy)]^{2+} + H^+$ | 2.78 | 2.15 |
| **(i = 3)** $[Ru^{III}(OH)(Hbpp)(trpy)]^{2+} \rightarrow [Ru^{III}(bpp)(OH)(trpy)]^+ + H^+$ | 5.43 | 6.58 |

It is noteworthy that oxidation from $Ru^{II}$ to $Ru^{III}$ greatly increases the acidity of the bonded water molecule, which becomes now more acidic than the pyrazolyl proton. Also remarkable is the relatively high $\Delta E_{1/2}$(IV/III–III/II) value (370 mV for **3a**) that is typical for Ru–aqua complexes with strong σ–donor ligands in their sphere of coordination such as acetylacetonate or our anionic bpp⁻ ligand, which stabilizes oxidation states III and IV.

The redox behavior of the pyridine complexes **4a** and **4b** is analogous to that of the aqua complexes but simplified by the fact that now there are only two sites of protonation and one redox process corresponding to the Ru(III/II) couple.

## D) Catalysis.

Cyclic voltammetry of **3a** at pH = 12 in the presence of benzyl alcohol shows that the $Ru^{IV}$=O species catalyzes the oxidation of the alcohol, presumably to benzaldehyde. Mathematical simulation of the process gives a second–order rate constant of 17.1 $M^{-1}$ $s^{-1}$.

## Synthesis and characterization of new ruthenium dimers with the bpp⁻ and trpy ligands. Application of $[Ru^{II}_2(bpp)(trpy)_2(H_2O)_2]^{3+}$ to water oxidation catalysis (PAPERS C–D).[3]

Water oxidation to molecular dioxygen, which takes place in natural photosynthesis, is attracting a great deal of attention in view of the decreasing energy resources and the environmental problems arising from the combustion of fossils fuels.

In spite of the big efforts performed by research groups from all over the world, only a handful of ruthenium and manganese complexes able to perform homogeneous water oxidation has been developed so far. As for the ruthenium complexes, they can be divided into two categories: mononuclear and dinuclear ammine complexes, and those containing a Ru–(μ–O)–Ru motif.

Among the former we encounter the most active catalyst reported up to date, i.e., $[(NH_3)_3Ru(\mu-Cl)_3Ru(NH_3)_3]^{2+}$ (with a pseudo–first–order rate constant for $O_2$ evolution, $k_{O2}$ $(s^{-1})$, of $5.6 \times 10^{-2}$). However, oxidation of the ammine ligands to $N_2$ occurs during the course of the catalysis, which is responsible for a very narrow range of linear behavior of the catalyst.
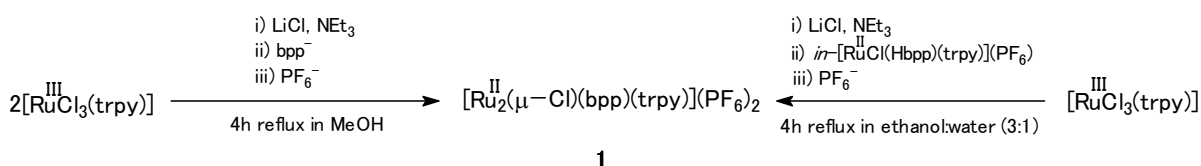
Among the ruthenium complexes containing the Ru–(μ–O)–Ru motif, a paradigmatic example is the already mentioned *blue dimer*, with a $k_{O2}$ value of $4.2 \times 10^{-3}$ $s^{-1}$. Multiple reports have appeared referring to its mechanism of action. It has been shown that the major pitfall of this type of catalysts is binding of anions present in solution to the high oxidation state species of the catalyst, which greatly slows down the overall catalysis

---

[3] (a) Sens, C.; Romero, I.; Rodríguez, M.; Llobet, A.; Parella, T.; Benet–Buchholz, J. *J. Am. Chem. Soc.* **2004**, *126*, 7798–7799. (b) Sens, C.; Rodríguez, M.; Romero, I.; Llobet, A.; Parella, T.; Benet–Buchholz, J. *To be submitted.*

because the rate-limiting step becomes water replacement of the coordinated anions, then inhibiting oxygen evolution.

Deprotonation of the Hbpp ligand in the previously described mononuclear complexes generates a coordination pocket that allows the formation of homo- and heterodinuclear systems. We decided to take advantage of this property to synthesize dinuclear Ru complexes. We were particularly interested in testing the capability of $[Ru^{II}_2(bpp)(trpy)_2(H_2O)_2]^{3+}$ to act as catalyst in water oxidation to molecular dioxygen.

Our first synthetic approach was to use the *in*-Cl monomer **2b** as starting material, refluxing it with one equivalent of $RuCl_3(trpy)$. A mixture of products was obtained that way, from which the μ-chloro dimer **1** was obtained in good yield (72.5 %), after some purification techniques. Similar yields of this compound (73.4 %) were also obtained by reacting two equivalents of $RuCl_3(trpy)$ with one equivalent of the deprotonated bpp⁻ ligand (**Scheme 1**). This latter route is more convenient, since preparation of the *in*-Cl **2b** is tedious and has a low overall performance.

$$2[\overset{III}{Ru}Cl_3(trpy)] \xrightarrow[\text{4h reflux in MeOH}]{\begin{array}{l}\text{i) LiCl, NEt}_3\\\text{ii) bpp}^-\\\text{iii) PF}_6^-\end{array}} [\overset{II}{Ru}_2(\mu-Cl)(bpp)(trpy)](PF_6)_2 \xleftarrow[\text{4h reflux in ethanol:water (3:1)}]{\begin{array}{l}\text{i) LiCl, NEt}_3\\\text{ii) }in\text{-}[\overset{II}{Ru}Cl(Hbpp)(trpy)](PF_6)\\\text{iii) PF}_6^-\end{array}} [\overset{III}{Ru}Cl_3(trpy)]$$

**1**

**Scheme 1.** Possible synthetic routes for the preparation of **1**.

The μ-acetato dimer, $[Ru^{II}_2(\mu-OAc)(bpp)(trpy)_2](PF_6)_2$ (**2**), is obtained in good yield when **1** is refluxed in the presence of an excess of sodium acetate. The bridging acetate is easily replaced by two aqua ligands in acidic aqueous media, generating $[Ru^{II}_2(bpp)(trpy)_2(H_2O)_2](PF_6)_3$ (**3**). The stability of **3** in this media, however, is limited, since replacement of the aqua ligands by the anions from the acid is observed in long-standing solutions. If the acid used to hydrolyze the μ-acetato bridge is $CF_3COOH$, then $[Ru^{II}_2(\mu-O_2CCF_3)(bpp)(trpy)_2](PF_6)_2$ (**4**) is generated.

Dimers **1**, **2** and **3** were thoroughly characterized by structural, spectroscopic and electrochemical techniques. Some of the distinctive features of the complexes that came from these studies are the following:

## A) X-ray diffraction.

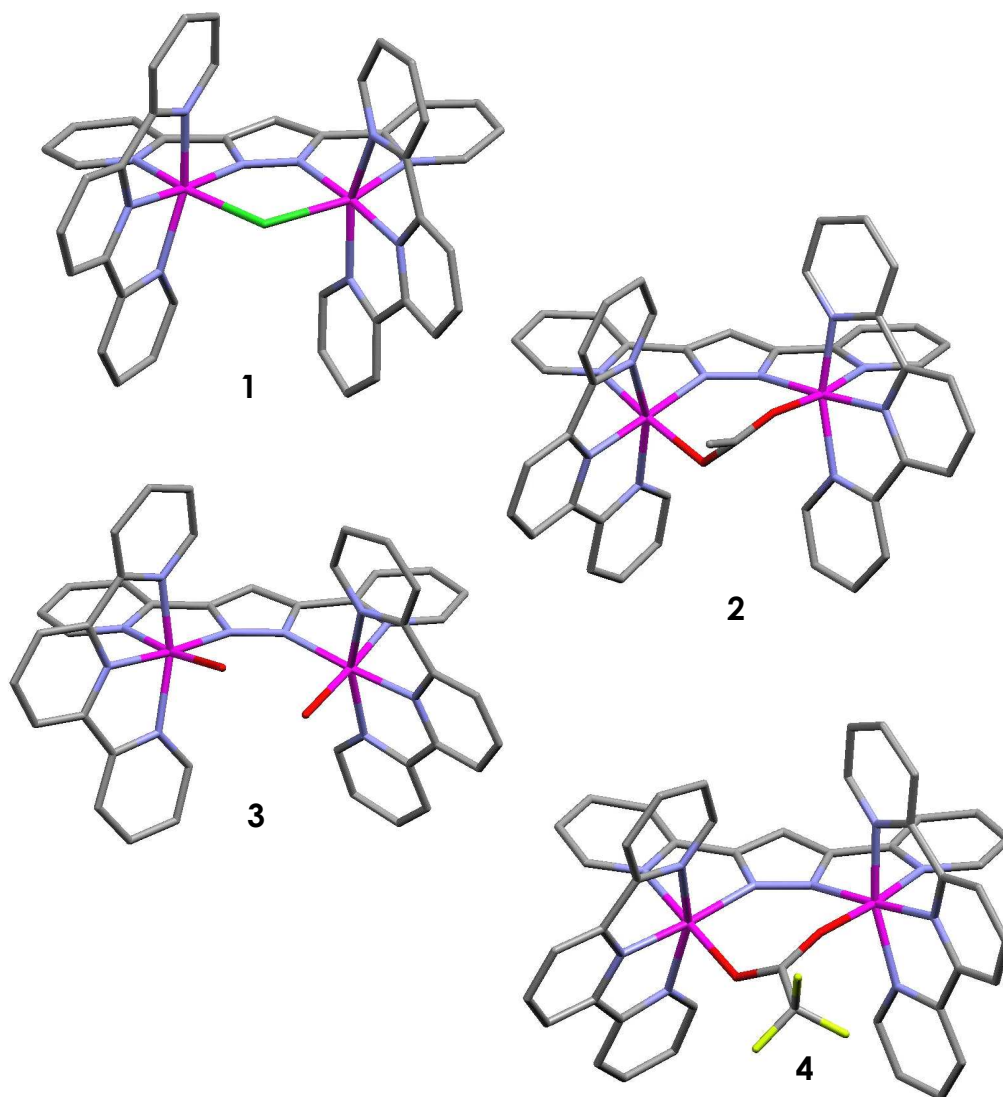The structures of complexes **1-4** have been solved by X-ray diffraction techniques and are shown in **Figure 12**.



**Figure 12.** X-ray diffraction structures for **1**, **2**, **3** and **4**.

## B) NMR spectroscopy.

The presence of a μ-acetato bridge in **2** is apparent in its ¹H-NMR spectrum by the appearance of a signal at 0.42 ppm, integrating 3 protons. This low δ value (compared to the 1.95 ppm signal for free acetate) is not surprising, since the methyl protons of the

acetate bridge are situated in the gap between the two trpy ligands and thus, affected by the π-electronic currents of their aromatic rings.

NMR spectra studies also served to unequivocally prove acidic hydrolysis of the bridging acetate. When one drop of CF$_3$COOH was added to a solution of **2** in D$_2$O, the 0.42 ppm signal was substituted by a new signal at 1.95 ppm, corresponding to free acetate.

## C) UV-vis spectroscopy.

The diaqua dimer **3** showed pH-dependent UV-vis spectra, in agreement with the acid-base properties of the coordinated water ligands. A spectrophotometric acid-base titration was performed that yielded a p$K_a$ of 6.70, corresponding to the one-proton deprotonation of one aqua ligand (**Figure 13**). This value contrasts with that of the related mononuclear complex *out*-[Ru$^{II}$(Hbpp)(trpy)(H$_2$O)]$^{2+}$, which is significantly higher (11.09). We attribute the increase in acidity of **3** to the formation of the highly stable {Ru$_2$O$_2$H$_3$} entity.
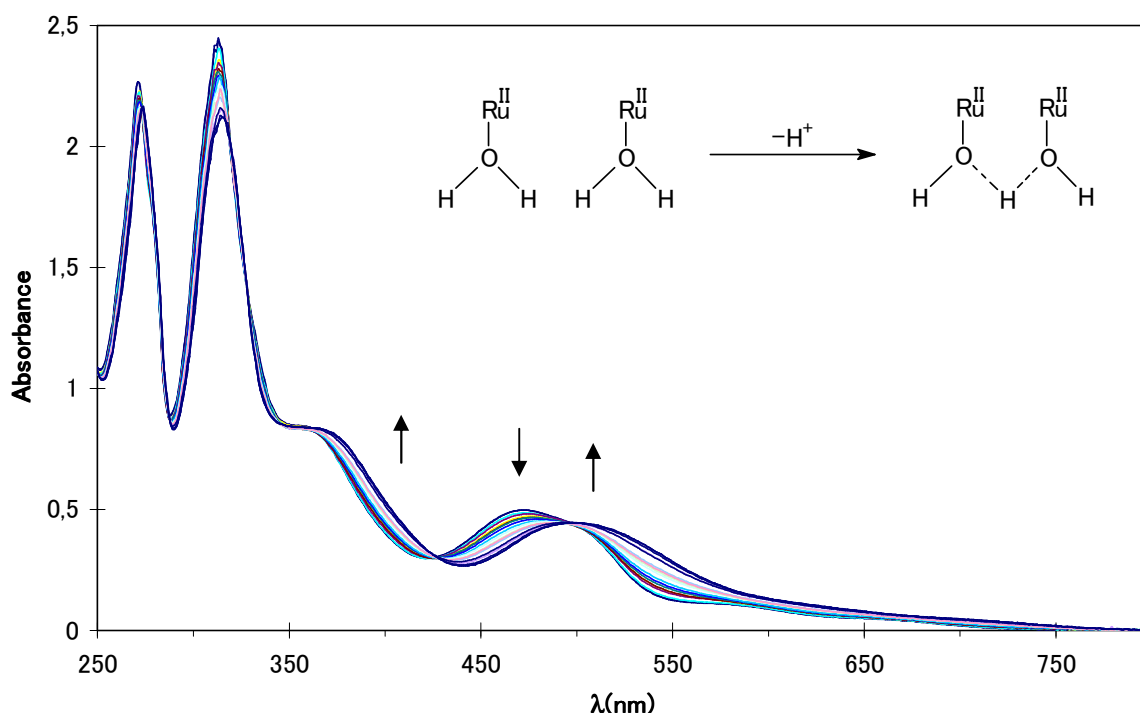


**Figure 13.** UV-vis spectral changes during the acid-base spectrophotometric titration of a 6.5 × 10$^{-5}$ M aqueous solution of **3** in 0.1 M CF$_3$COOH. The pH of the solution was adjusted by adding small volumes (approx. 10 μL) of 4 M NaOH in order to produce a negligible overall volume change.

## D) Electrochemistry.

Cyclic voltammetry studies of **1**, **2** and **3** in dichloromethane show the presence of two waves corresponding to the one-electron oxidations from $Ru^{II,II}$ to $Ru^{II,III}$ and from $Ru^{II,III}$ to $Ru^{III,III}$ (**Figure 14**). The approx. 300 mV separation between these waves indicates that the two metal centers are strongly coupled.
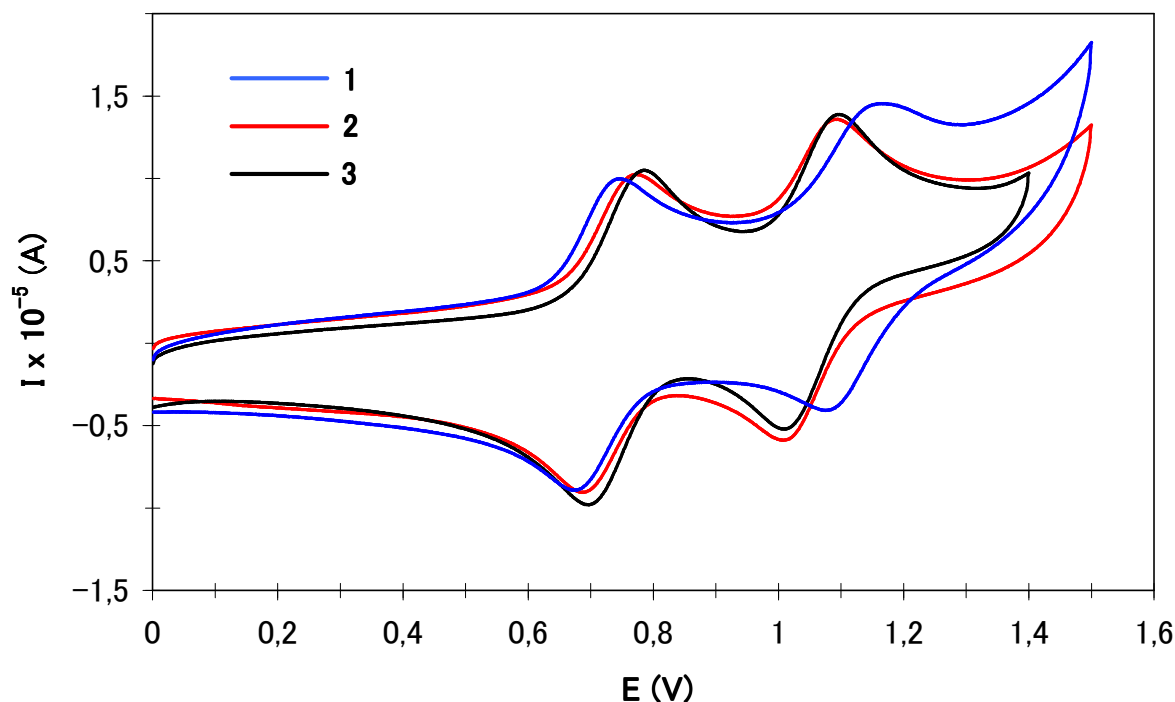


**Figure 14.** Cyclic voltammetries for 1 mM **1**, **2** and **3** in $CH_2Cl_2$.

As for **3**, its pH-dependent redox behavior was evidenced in aqueous solution. The CV of **3** in aqueous acid at pH = 1, where replacement of the acetato bridge by two aqua ligands takes place, exhibits three waves at 0.54, 0.61 and 0.84 V which correspond to one-electron oxidation processes from $Ru^{II}Ru^{II}$ to $Ru^{III}Ru^{IV}$ (as confirmed by coulombimetric studies). A fourth anodic peak is also observed at $E_{p,a}$ = 1.05 V that is assigned to the oxidation from $Ru^{III}Ru^{IV}$ to $Ru^{IV}Ru^{IV}$. The corresponding cathodic peak is not visible in the reverse scan, indicating that $Ru^{IV}Ru^{IV}$ is not stable on the time scale of the cyclic voltammetry. We anticipated that it could be due to water oxidation, which was confirmed in a bulk experiment. The Pourbaix diagram of **3** (**Figure 15**) shows its rich redox chemistry; different oxidation states with different degrees of protonation are accessible
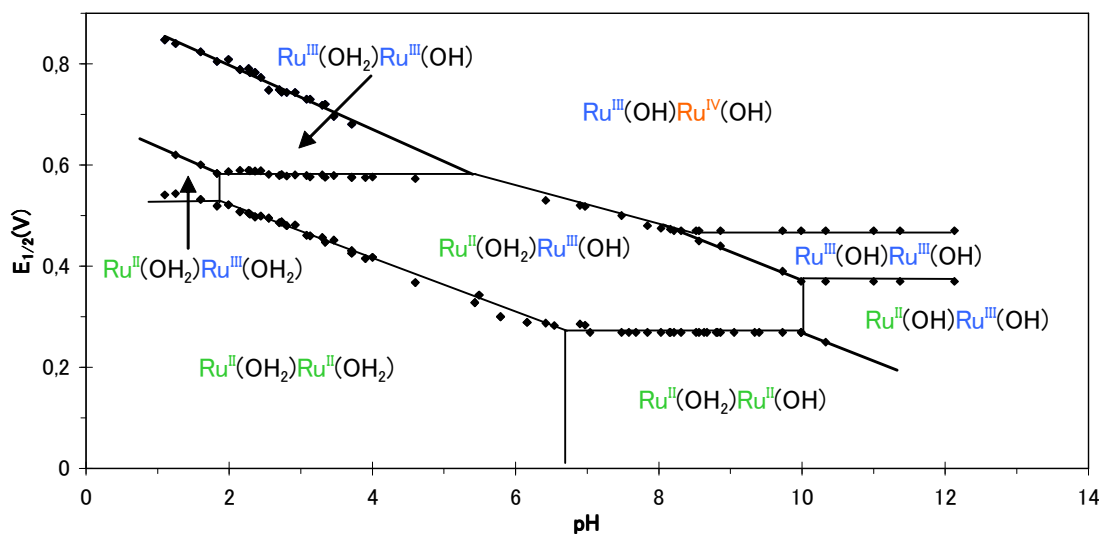
within a narrow potential range.



**Figure 15.** Pourbaix diagram for **3**. The pH−potential regions of stability for the various oxidation states and their dominant proton compositions are indicated. The p$K_a$ values are shown by the vertical solid lines in the various E−pH regions.

## E) Catalysis.

The capability of **3** in water oxidation was tested by adding 100 to 300−fold molar excesses of $Ce^{IV}$ to $1.65 \times 10^{-6} - 3.48 \times 10^{-6}$ mols of $Ru^{II,II}$ dimer in 0.1 M $CF_3SO_3H$. Oxygen evolution clearly demonstrated that **3** is an active catalyst, with an efficiency of 73% (based on the amount of $Ce^{IV}$ added) and 18.6 metal cycles when $1.83 \times 10^{-6}$ mols of the dimer were mixed with 100 equivalents of $Ce^{IV}$. Heterogeneous water oxidation in a Nafion membrane was also tested, but the yields of $O_2$ attained with this system were significantly decreased.

According to the structure of **3**, where the two Ru−$OH_2$ moieties are situated in close proximity in the gap between the two bulky trpy ligands, it seemed that an intramolecular pathway was the most plausible mode of operation of the catalyst, as indicated in **Scheme 2**.
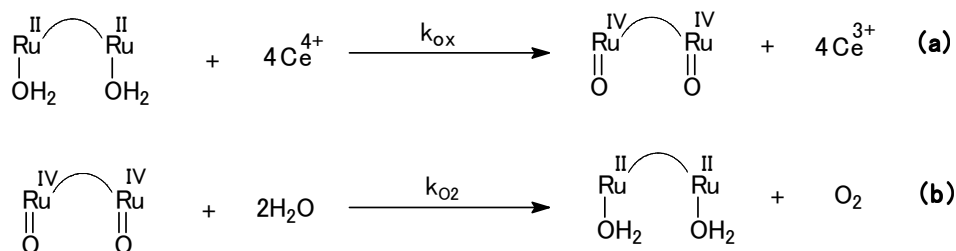
**Scheme 2.** Proposed pathway for water oxidation by **3**.

This model was further supported by kinetic studies using large excesses of $Ce^{IV}$ (so that reaction **(b)** was the rate-determining step). They showed that the initial $O_2$ evolution rate, $\upsilon_{O2}$ (mol s$^{-1}$), obtained from the initial slope at time zero of the plots of mols of $O_2$ evolved *vs.* time, increased linearly with complex concentration at low concentration values, indicating that four-electron water oxidation is catalyzed by one molecule of the complex (**Figure 16**).
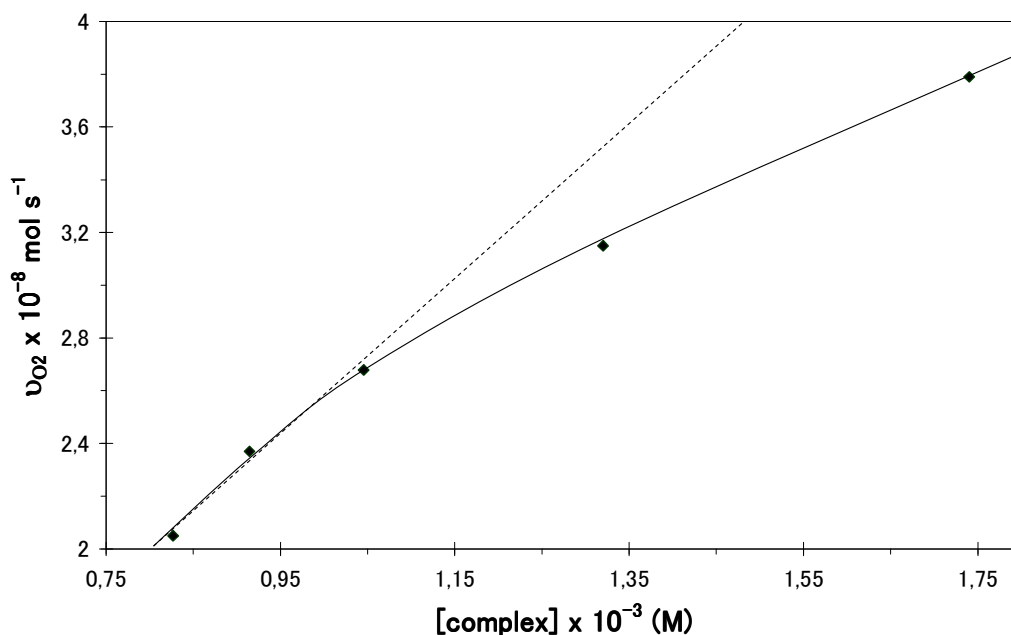


**Figure 16.** Plot of initial $O_2$ evolution rates, $\upsilon_{O2}$ (mols s$^{-1}$), *vs.* complex concentration in an aqueous 0.1 M $CF_3SO_3H$ solution.

The pseudo-first-order rate constant for $O_2$ evolution, $k_{O2}$ (s$^{-1}$), was obtained from kinetic analysis under large excess of $Ce^{4+}$ as $1.4 \times 10^{-2}$. This value makes our complex one of the most effective catalysts reported up to date and the first well characterized ruthenium

dimer that is not based on a Ru–(μ–O)–Ru moiety able to perform this catalysis.

We attribute the effectiveness of this compound to the following factors: (a) the anionic bpp⁻ is a rigid ligand which forces the two Ru–OH$_2$ moieties to stay in close proximity, thus favoring a proper orientation of the Ru=O groups; (b) the absence of an oxo–bridge, when compared to the *blue dimer*, thus avoiding decomposition by reductive cleavage and by the strong thermodynamic force to *trans*–dioxo formation, and (c) the bpp– is an anionic ligand and thus, reduces the overall charge of the active catalyst, increasing its stability towards competing anation side reactions, which have been reported to deactivate the *blue dimer*.

Dimer **3**, however, still suffers from deactivation pathways that limit its effectiveness. We are currently trying to elucidate such pathways in order to design more robust water oxidation catalysts.

# CONCLUSIONS

## PAPER A

▸ Two new mononuclear Ru complexes, **2a** and **2b**, have been prepared from [RuCl$_2$(dmso)$_4$] and Hbpp. The fact that only three (**2a** and the pair of enantiomers **2b**) from the six possible stereoisomers are obtained from this reaction, has been rationalized in terms of structural and electronic factors, particularly the intramolecular hydrogen bond between the inner dmso and the aminic proton of Hbpp.

▸ **2a** and **2b** have been structurally, spectroscopically and electrochemically characterized. In acetonitrile basic media, **2a** has proven to undergo linkage isomerization reactions of one dmso ligand when going from Ru$^{II}$ to Ru$^{III}$. The kinetic and thermodynamic constants for this process have been determined by means of cyclic voltammetry.

▸ Irradiation of either **2a** or **2b** with UV or sunlight provokes the replacement of one dmso by an acetonitrile molecule so that **4** is formed. This complex has been characterized in solution by spectroscopic and electrochemical techniques. The fact that only one of the two dmso ligands is substituted, compared to related systems where two successive substitutions of dmso for MeCN take place, suggests that the inner dmso is much more stable due to the hydrogen bond with the aminic proton of Hbpp.

▸ **2a** and **2b** have proven to be active catalysts in the hydrogen transfer from 2-propanol to acetophenone, yielding 2-phenylethyl alcohol as the only product and 42.1% conversion (36.1 metal cycles) at 80 °C for **2a**, which is markedly more efficient than **2b**.

## PAPER B

▸ Two geometrical chloro isomers, **2a** and **2b**, are obtained from the reaction of *cis(out),cis*–[RuCl$_2$(Hbpp)(dmso)$_2$] (paper A, **2b**) and trpy. Better yields of these

complexes can be obtained by a different route which uses $[RuCl_3(trpy)]$ and bpp–BOC as starting materials. These compounds have been isolated and characterized by means of structural, spectroscopic and electrochemical techniques.

▸ **2a** and **2b** have been used as starting materials for the synthesis of the analogous aqua (**3a**, **3b**) and pyridine (**4a**, **4b**) complexes, which have also been isolated and characterized.

▸ The acid–base properties of the aqua complexes, **3a** and **3b**, and the pyridyne complex **4a** have been thoroughly investigated by cyclic voltammetry (Pourbaix diagram) and acid–base spectrophotometric titrations. Mathematical treatment of the experimental data thus obtained has allowed us to determine the $pK_a$ values for the different protonation equilibria of the complexes in oxidation states II and III.

▸ **3a** has been shown to be a good catalyst in the electrochemical oxidation of benzyl alcohol, presumably to benzaldehyde. The second–order rate constant for the process has been determined as 17.1 $M^{-1}$ $s^{-1}$ by mathematical simulation.

# PAPERS C–D

▸ Two different synthetic routes have been used to prepare the μ–chloro dimer **1** in good yield. The μ–acetato dimer **2** has been obtained from **1** and excess sodium acetate. The diaqua complex **3** has been prepared from either basic hydrolysis of **1** or acid hydrolysis of **2**. These complexes have been characterized by means of structural, spectroscopic and electrochemical techniques.

▸ Long–standing solutions of the diaqua dimer **3** in acidic media have proven to be unstable to coordination of anions from the solution. Crystals of the μ–trifluoroacetato dimer **4** has been obtained in acidic $CF_3COOH$ media after some days.

▸ The acid–base properties of the diaqua dimer **3** have been thoroughly investigated by cyclic voltammetric and bulk electrolysis experiments, and the corresponding Pourbaix diagram obtained. The $pK_a$ for the one–proton deprotonation of one aqua ligand has been determined by acid–base spectrophotometric titration as 6.7. This low $pK_a$ value

is attributed to the formation of the highly stable $\{Ru_2O_2H_3\}$ entity.

▸ The UV–vis spectra for the different oxidation states of **3**, from $Ru^{II}Ru^{II}$ to $Ru^{III}Ru^{IV}$, have been obtained by either chemical or electrochemical oxidation of the complex. UV–vis kinetic studies on the stepwise oxidation from $Ru^{II,II}$ to $Ru^{IV,IV}$ have been performed, and the individual second–order rate constants for the different oxidation processes determined.

▸ The capability of **3** in water oxidation to molecular dioxygen has been investigated in homogeneous solution using $Ce^{IV}$ as oxidant. Oxygen evolution has been clearly demonstrated by gas chromatography. An efficiency of 73% and 18.6 metal cycles were obtained using $1.83 \times 10^{-6}$ of dimer and 100–fold molar excess of cerium. This complex has also been shown to catalyze water oxidation in a heterogenous Nafion membrane, but the yields of $O_2$ evolution are lower.

▸ An intramolecular pathway for the water oxidation process has been proposed. It involves the four–electron oxidation of the $Ru^{II,II}$ dimer to the $Ru^{IV,IV}$ complex that reverts to the $Ru^{II,II}$ oxidation state upon releasing of molecular dioxygen. This model is consistent with kinetic studies on the evolution of oxygen as a function of catalyst and cerium concentrations, performed in homogeneous acidic solution, which show that the four–electron oxidation of water is catalyzed by one molecule of complex under large excesses of cerium.

▸ The pseudo–first–order rate constant for oxygen evolution has been calculated as $1.4 \times 10^{-2}$ $s^{-1}$, which is among the highest values reported up to date. Unfortunately, the diaqua dimer **3** is deactivated during the catalysis to yield an orange species which we are currently trying to characterize.